The Astrophysical Journal, 777:95 (19pp), 2013 November 10 doi:10.1088/0004-637X/777/2/95

BIOSIGNATURE GASES IN H_2-DOMINATED ATMOSPHERES ON ROCKY EXOPLANETS

S. Seager[1,2], W. Bains[1,3], and R. Hu[1]
[1] Department of Earth, Atmospheric, and Planetary Sciences, Massachusetts Institute of Technology, 77 Massachusetts Avenue, Cambridge, MA 02139, USA
[2] Department of Physics, Massachusetts Institute of Technology, 77 Massachusetts Avenue, Cambridge, MA 02139, USA
[3] Rufus Scientific Ltd., 37 The Moor, Melbourn, Herts SG8 6ED, UK
Received 2013 April 2; accepted 2013 August 13; published 2013 October 18

ABSTRACT

Super-Earth exoplanets are being discovered with increasing frequency and some will be able to retain stable H_2-dominated atmospheres. We study biosignature gases on exoplanets with thin H_2 atmospheres and habitable surface temperatures, using a model atmosphere with photochemistry and a biomass estimate framework for evaluating the plausibility of a range of biosignature gas candidates. We find that photochemically produced H atoms are the most abundant reactive species in H_2 atmospheres. In atmospheres with high CO_2 levels, atomic O is the major destructive species for some molecules. In Sun-Earth-like UV radiation environments, H (and in some cases O) will rapidly destroy nearly all biosignature gases of interest. The lower UV fluxes from UV-quiet M stars would produce a lower concentration of H (or O) for the same scenario, enabling some biosignature gases to accumulate. The favorability of low-UV radiation environments to accumulate detectable biosignature gases in an H_2 atmosphere is closely analogous to the case of oxidized atmospheres, where photochemically produced OH is the major destructive species. Most potential biosignature gases, such as dimethylsulfide and CH_3Cl, are therefore more favorable in low-UV, as compared with solar-like UV, environments. A few promising biosignature gas candidates, including NH_3 and N_2O, are favorable even in solar-like UV environments, as these gases are destroyed directly by photolysis and not by H (or O). A more subtle finding is that most gases produced by life that are fully hydrogenated forms of an element, such as CH_4 and H_2S, are not effective signs of life in an H_2-rich atmosphere because the dominant atmospheric chemistry will generate such gases abiologically, through photochemistry or geochemistry. Suitable biosignature gases in H_2-rich atmospheres for super-Earth exoplanets transiting M stars could potentially be detected in transmission spectra with the *James Webb Space Telescope*.

Key words: astrobiology – planets and satellites: atmospheres

Online-only material: color figures

1. INTRODUCTION

The detection of exoplanet atmospheric biosignature gases by remote sensing spectroscopy is usually taken as inevitable for the future of exoplanets. This sentiment is being borne out with the discovery of increasing numbers of smaller and lower-mass planets each year. In addition, the development of larger and more sophisticated telescopes (such as the *James Webb Space Telescope* (*JWST*) slated for launch in 2018; Gardner et al. 2006) and the giant 20 m to 40 m class ground-based telescopes[4] continues to fuel the concept that the eventual detection and study of biosignature gases is a near certainty.

The topic of biosignature gases, however, may remain a futuristic one unless a number of extreme challenges can be overcome. The biggest near-term challenge is to find a large enough pool of potentially habitable exoplanets accessible for follow up atmospheric study.[5] By potentially habitable, we mean rocky planets with surface liquid water and not those with massive envelopes making any planet surface too hot for the complex molecules required for life. A large pool of such planets is needed because there could be a large difference in the numbers of seemingly potentially habitable planets (based on their measured host stellar type, orbit, mass or size, and inferred surface temperature) and those that are inhabited by life that produces useful biosignature gases (which will be inferred from measured atmospheric spectra). Useful biosignature gases mean those that can accumulate in the planet atmosphere, are spectroscopically active, and are not overly contaminated by geophysical false positives. A contemporary, related point to identifying a large enough pool of planets is that even the fraction of small or low-mass planets that are potentially habitable—that is, with surface conditions suitable for liquid water—is not yet known. The reason is that the factors controlling a given planet's surface temperatures are themselves not yet observed or known, including the atmosphere mass (and surface pressure), the atmospheric composition, and hence the concomitant greenhouse gas potency (see the review by Seager 2013).

A second major challenge for the study of biosignature gases is the capability of telescopes to robustly detect molecules in terrestrial exoplanet atmospheres. This challenge is continuously faced in today's hot Jupiter atmosphere studies (e.g., Seager 2010), where many atmospheric molecular detections based on data from the *Hubble Space Telescope* (*HST*) or the *Spitzer Space Telescope* remain controversial (see Deming et al. 2013 and references therein). For transiting planets, the ability to identify and remove systematics to a highly precise level while adding together numerous transit events from different epochs is a necessity to reach the small signals of terrestrial planet atmospheres. For directly imaged planets, the ability to reach down to Earth-sized planets in Earth-like orbits is one of the most substantial technological challenges to ever face astronomers.

[4] The Extremely Large Telescope (http://www.eso.org/public/teles-instr/e-elt.html), the Giant Magellan Telescope (http://www.gmto.org/), and the 30 m Telescope (http://www.tmt.org/).
[5] For example, the all-sky, space-based TESS mission (Transting Exoplanet Planet Survey Satellite, PI: George Ricker) has been selected under NASA's Astrophysics Explorer Program for launch in 2017.

While technological development is ongoing, there are as of yet no solid plans to launch a space telescope capable of directly imaging terrestrial-size planets.

A third major challenge in the study of biosignature gases has to do with geological false positive signatures. These false positives are gases that are produced geologically and emitted by volcanos or vents in the crust or ocean. Geochemistry has the same chemicals to work with that life does, and therefore false positives are inevitable. While early theoretical studies favored detection of redox disequilibrium (such as O_2 and CH_4) that should not both exist in an atmosphere in photochemical steady state, often one molecule of the set is too weak for potential detection spectroscopically. The conventionally adopted approach (at least in theoretical studies) is therefore to identify a biosignature gas that is many orders of magnitude out of thermodynamic equilibrium with the expected gas composition of the atmosphere and to study the gas in the context of the planet atmosphere environment via atmospheric spectra that cover a wide wavelength range. A more likely outcome of the field of biosignature gases will be to develop a probabilistic assessment of the likelihood a molecule in a given atmosphere can be attributed to life, because spectroscopic data and the information for a complete assessment of the planetary environment will be limited.

To increase the chances of detecting exoplanet atmospheric biosignature gases, we are motivated to widen the parameter space of types of planets where biosignature gases can accumulate and should be sought out observationally. We here describe, for the first time to our knowledge, the case for and against biosignature gases in hydrogen-rich atmospheres. Some massive enough or cold enough super-Earths (loosely defined as planets with up to 10 Earth masses) will be able to retain hydrogen in their atmospheres (see the discussion in Section 5.2). In general, planets are expected to outgas or capture hydrogen from the nebula during planet formation. Here, we are concerned with super-Earths with relatively thin hydrogen atmospheres and not planets with massive atmospheres or envelopes (as in mini-Neptunes), which will have surfaces too hot for liquid water (L. Rogers & S. Seager, in preparation) or may not even have a surface. A thin hydrogen atmosphere does not add much to either the mass or the size of the planet (Adams et al. 2008), so that an H_2-rich atmosphere itself does not aid in planet discovery or detection.

Super-Earths with H_2-rich atmospheres are nonetheless in some ways more favorable for detection and study than their terrestrial planet counterparts with N_2- or CO_2-dominated atmospheres. A more massive planet than Earth (i.e., more likely to retain atmospheric H_2 than Earth) is easier to discover than an Earth-mass planet via the radial velocity technique. A more massive planet than Earth is also larger and so easier to discover or detect by the transit technique than a lower mass planet. For example a 10 $M_\oplus$ planet of Earth-like composition would have a radius 1.75 times larger than that of the Earth (e.g., Seager et al. 2007). The larger planet area is more favorable for atmosphere study in reflected or thermally emitted radiation than an Earth-sized planet. For transit transmission spectra, planets with H_2-rich atmospheres have a much larger signal compared with H-poor atmospheres because of the larger scale height H, based on the mean molecular weight μ (e.g., Seager 2010):

$$H = \frac{kT}{\mu m_H g}, \quad (1)$$

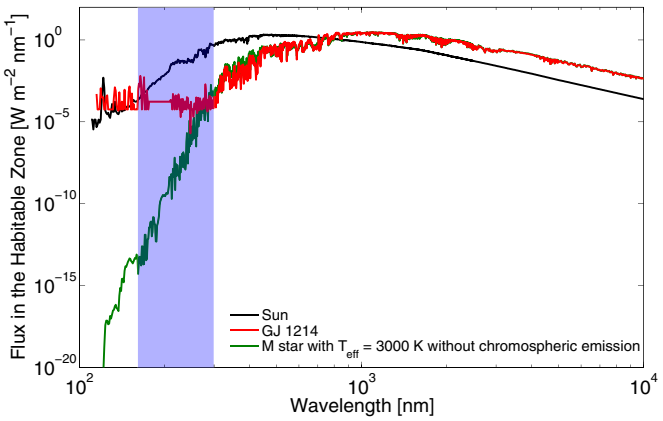

Figure 1. Comparison of stellar fluxes. The radiative fluxes received by a planet in the habitable zone of a solar-like star, a weakly active M dwarf star (like GJ 1214), and a theoretically simulated quiet M dwarf star with an effective temperature of 3000 K with no chromospheric emission are shown. The flux is scaled so that the planet has a surface temperature of 290 K. The spectrum of the Sun-like star is from the Air Mass Zero reference spectrum during a solar quiet period (http://rredc.nrel.gov/solar/spectra/am0/). The spectrum of GJ 1214 contains two parts: for wavelengths shorter than 300 nm, we take the most recent *HST* measurement (France et al. 2013); for wavelengths longer than 300 nm, we take the NextGen simulated spectrum for an M dwarf star having parameters closest to those of GJ 1214 (i.e., an effective temperature of 3000 K, surface gravity $\log(g) = 5.0$, and metallicity [M/H] = 0.5). The spectrum with no chromospheric emission is also from the NextGen model (Allard et al. 1997). Under the common definition of weakly active, or relatively quiet M dwarf, the UV environment in its habitable zone can differ by more than six orders of magnitude.

(A color version of this figure is available in the online journal.)

where k is Boltzmann's constant, T is temperature, m_H is the mass of the hydrogen atom, and g is the surface gravity. The point is that when H_2 dominates the atmospheric composition over the terrestrial planet atmosphere gases CO_2 and N_2, the mean molecular weight is ~20 times smaller and hence the scale height is ~20 times larger. The observational imprint of an atmosphere is usually taken as about $5H$.

Turning back to biosignature gases, they have been studied theoretically as indicators of life on planets with oxidized atmospheres for over half a century, beginning with Lederberg (1965) and Lovelock (1965). One highlight from the last decade is the realization that low-UV radiation environments compared with solar radiation environments lead to a much higher concentration of biosignature gases, as studied for Earth-like planet atmospheres. This is because the stellar UV creates the radical OH (in some cases O) that destroys many gases in the atmosphere and thus reduces the gas lifetime. A low-UV radiation environment is taken to be that of a planet orbiting a UV-quiet M dwarf star (see Figure 1 and discussion in Section 5.6) A second highlight in biosignature gas research in the last decade is the theoretical exploration of potential biosignature gases beyond the conventionally considered dominant Earth or early Earth-based ones of O_2, O_3, N_2O, and CH_4. The variations studied include dimethylsulfide (DMS; Pilcher 2003), methyl chloride (CH_3Cl; Segura et al. 2005), and other sulfur compounds including CS_2 and COS (Domagal-Goldman et al. 2011). We refer the reader to Seager et al. (2012) for a review, Seager et al. (2013) for a biosignature gas classification scheme, and Seager et al. (2013) for a biomass model estimate intended as a plausibility check to consider biosignature gas surface fluxes different from Earth values.

We begin with a description of our atmosphere and biomass estimate model in Section 2. We present general results in

Section 3 and specific results for a number of potential and unlikely biosignature gases in Section 4. A discussion in Section 5 is followed by a summary and conclusion in Section 6.

2. MODEL

The model goal is to computationally generate atmospheric spectra for exoplanets with H_2-rich atmospheres with biosignature gases. The model consists of a photochemistry code that takes biosignature gases as surface fluxes, an approximate temperature profile calculation, and a line-by-line spectral calculation (Seager et al. 2013; Hu et al. 2012). The model also uses a biomass model estimate to check whether or not a biosignature gas could be the result of a plausible surface ecology.

2.1. Model Atmosphere

Photochemistry Model. The focus on chemistry is critical for biosignature gases because sinks control a biosignature gas lifetime and hence the gas' potential to accumulate in the planetary atmosphere. A model for atmospheric chemistry is required to connect the amount of biosignature gas in the atmosphere (as required for detection) to the biosignature source flux at the planetary surface.

Our photochemical model is presented in Hu et al. (2012). The photochemical code computes the steady-state chemical composition of an exoplanetary atmosphere. The system can be described by a set of time-dependent continuity equations, one equation for each species at each altitude. Each equation describes chemical production, chemical loss, eddy diffusion and molecular diffusion (contributing to production or loss), sedimentation (for aerosols only), emission and dry deposition at the lower boundary, and diffusion-limited atmospheric escape for light species at the upper boundary. The code includes 111 species, 824 chemical reactions, and 71 photochemical reactions. Starting from an initial state, the system is numerically evolved to the steady state in which the number densities no longer change.

The generic model computes chemical and photochemical reactions among all O, H, N, C, and S species and the formation of sulfur and sulfate aerosols. The numerical code is designed to have the flexibility of choosing a subset of species and reactions in the computation. The code therefore has the ability to treat both oxidized and reduced conditions by allowing the selection of "fast species." For the chemical and photochemical reactions, we use the most up-to-date reaction rate data from both the NIST database (http://kinetics.nist.gov) and the JPL publication (Sander et al. 2011). Ultraviolet (UV) and visible radiation in the atmosphere is computed by the δ-Eddington two-stream method with molecular absorption, Rayleigh scattering, and aerosol Mie scattering contributing to the optical depth. The model was developed from the ground-up and has been tested and validated by reproducing the atmospheric composition of Earth and Mars (Hu et al. 2012; Hu 2013).

For biosignature gases that are minor chemical perturbers in the atmosphere, the biosignature lifetime can be estimated based on the abundance of the major chemical sink. For this paper, the values of NH_3 and N_2O surface source fluxes are calculated from the full photochemistry model, whereas the calculations of surface source fluxes for other biosignature gases are simplified estimates. One more point to note is that photochemistry is relatively high in the atmosphere, typically above mbar levels, where stellar UV radiation can penetrate from above.

Temperature–Pressure Profile. The precise temperature-pressure structure of the atmosphere is less important than photochemistry for a first-order description of biosignatures in H_2-rich atmospheres. The reason is that most biosignature gases of interest have sources and sinks that are not significantly affected by minor deviations in the temperature pressure profile. Moreover, the biosignature gases themselves are secondary players in governing the heating structure of the atmosphere.

We therefore justify using the photochemistry model in a stand-alone mode, with a pre-calculated temperature–pressure profile. The calculated temperature–pressure profile is approximate and is one that assumes a surface temperature (i.e., 290 K), an appropriate adiabatic lapse rate for H_2-rich compositions, and a constant temperature above the convective layer of the atmosphere. Such assumed temperature profiles are consistent with greenhouse warming in the troposphere and a lack of UV absorbers in the stratosphere. The semi-major axis of the planet is then derived based on the assumed temperature profile by balancing the energy flux of incoming stellar radiation and outgoing planetary thermal emission. The details of this procedure are described in Hu et al. (2012).

Synthetic Spectra. To generate exoplanet transmission and thermal emission spectra, we use a line-by-line radiative transfer code (Seager et al. 2000; Madhusudhan & Seager 2009; Hu et al. 2012). Opacities are based on molecular absorption with cross sections computed based on data from the HITRAN 2008 database (Rothman et al. 2009), molecular collision-induced absorption when necessary (e.g., Borysow 2002), Rayleigh scattering, and aerosol extinction computed based on Mie theory. The atmospheric transmission is computed for each wavelength by integrating the optical depth along the limb path (as outlined in, e.g., Seager & Sasselov 2000; Miller-Ricci et al. 2009). The planetary thermal emission is computed by integrating the radiative transfer equation without scattering for each wavelength (e.g., Seager 2010).

We consider clouds in the emergent spectra for thermal emission by considering 50% cloud coverage by averaging cloudy and cloud-free spectra. We omit clouds for the transmission spectra model because the clouds are at low altitudes whereas the spectral features form at high altitudes.

2.2. Biomass Model Estimates

A biomass model estimate has been developed by Seager et al. (2013) that ties biomass surface density to a given biosignature gas surface source flux. The motivating rationale is that with a biomass estimate, biosignature gas source fluxes can be free parameters in model predictions and therefore provide a physical plausibility check in terms of reasonable biomass. The approach aims to enable consideration of a wide variety of both gas species and their atmospheric concentration in biosignature model predictions. The biomass model estimates are valid to one or two orders of magnitude. We provide a summary of the biomass model here with the full details available in Seager et al. (2013).

The biomass model is used in the following algorithm. First, we calculate the amount of biosignature gas required to be present at "detectable" levels in an exoplanet atmosphere from a theoretical spectrum (we define a detection metric in Section 2.3). Second, we determine the gas source flux necessary to produce the atmospheric biosignature gas in the required atmospheric concentration. The biosignature gas atmospheric concentration is a function not only of the gas surface source flux, but also of other atmospheric and surface sources and sinks.

Third, we estimate the biomass that could produce the necessary biosignature gas source flux. Fourth, we consider whether the estimated biomass surface density is physically plausible, by comparison with maximum terrestrial biomass surface density values and total plausible surface biofluxes.

Based on life on Earth, a summary overview is that a biomass surface density of 10 g m^{-2} is sensible, 100 g m^{-2} is plausible, and 5000 g m^{-2} is possible. In real situations, the total biomass is nearly always limited by energy, bulk nutrients (carbon, nitrogen), trace nutrients (iron, etc.), or all three. Regarding global surface biofluxes, we provide values and references where needed in our results and discussion.

The biomass model estimates are tied to the type of biosignature gas and so we briefly summarize our biosignature classification scheme before discussing each biomass model estimate.

Type I biosignature gases are generated as by-product gases from microbial energy extraction. For example, on Earth, many microbes extract energy from chemical energy gradients using the abundant atmospheric O_2 for aerobic oxidation:

$$X + O_2 \rightarrow \text{oxidized X}. \quad (2)$$

H_2O is generated from H_2, CO_2 from organics, SO_2 or SO_4^{2-} from H_2S, rust from iron sulfide (FeS), NO_2^- and NO_3^- from NH_3, etc.

On an exoplanet with an H_2-rich atmosphere, the abundant reductant would now be atmospheric H_2 such that

$$H_2 + X \rightarrow \text{reduced X}. \quad (3)$$

The oxidant must come from the interior.

In other words, for chemical potential energy gradients to exist on a planet with an H_2-rich atmosphere, the planetary crust must (in part) be oxidized in order to enable a redox couple with the reduced atmosphere. The by-product is always a reduced gas, because in a reducing environment H_2-rich compounds are the available reductants. To be more specific, oxidants would include gases such as CO_2 and SO_2.

The Type I biosignature gas biomass model is based on thermodynamics and is derived from conservation of energy and discussed in detail in Seager et al. (2013). The biomass model estimate is

$$\Sigma_B \simeq \Delta G \left[\frac{F_{\text{source}}}{P_{m_e}} \right]. \quad (4)$$

Here, Σ_B is the biomass surface density in g m^{-2} and ΔG is the Gibbs free energy of the chemical redox reaction from which energy is extracted (i.e., Equation (2)). ΔG depends on the standard free energy of reaction (ΔG_0) and the concentration of the reactants and products. Reactant and product concentrations can include ocean pH (concentration of H^+) in reactions that generate or consume protons. ΔG_0 values are taken from Amend & Shock (2001).

The term P_{m_e} is an empirically determined microbial maintenance energy consumption rate that is the minimum amount of energy an organism needs per unit time to survive in an active state (i.e., a state in which the organism is ready to grow). An empirical relation has been identified by Tijhuis et al. (1993) that follows the Arrhenius law

$$P_{m_e} = A \exp \left[\frac{-E_A}{RT} \right]. \quad (5)$$

Here, $E_A = 6.94 \times 10^4$ kJ mol^{-1} is the activation energy, $R = 8.314$ kJ mol^{-1} K^{-1} is the universal gas constant, and T in units of K is the temperature. The constant A is 4.3×10^7 kJ g^{-1} s^{-1} for aerobic growth and 2.5×10^7 kJ g^{-1} s^{-1} for anaerobic growth (Tijhuis et al. 1993). Here, per g refers to per g of the wet weight of the organism. P_{m_e} is in units of kJ g^{-1} s^{-1}.

The free parameter in this biomass model estimate (Equation (4)) is the biosignature gas source flux F_{source} (in units of mole m^{-2} s^{-1}). F_{source} is the flux of the metabolic by-product and is also the surface bioflux required to generate a given biosignature gas concentration in the atmosphere.

Type II biosignature gases are by-product gases produced by the metabolic reactions for biomass building and require energy. On Earth, these are reactions that capture environmental carbon (and, to a lesser extent, other elements) in biomass. Type II biosignature reactions are energy-consuming and on Earth the energy comes from sunlight via photosynthesis.

There is no useful biomass model for Type II biosignature gases because once the biomass is built a Type II biosignature gas is no longer generated.

Type III biosignature gases are produced by life but not as by-products of their central chemical functions. Type III biosignature gases appear to be particular to specific species or groups of organisms and require energy for their production. Because the chemical nature and amount released for Type III biosignature gases are not linked to the local chemistry and thermodynamics, the Type III biosignature gas biomass model is an estimate based on lab culture production rates.

We estimate the biomass surface density by taking the biosignature gas source flux F_{source} (in units of mole m^{-2} s^{-1}) divided by the mean gas production rate in the lab R_{lab} (in units of mole g^{-1} s^{-1}):

$$\Sigma_B \simeq \frac{F_{\text{source}}}{R_{\text{lab}}}. \quad (6)$$

We take the maximum observed for the Type III R_{lab} rates from different studies (Seager et al. 2013). The caveat of the Type III biomass estimate explicitly assumes that the range of R for life on exoplanets is similar to that for life in Earth's lab environment. Nonetheless, we have showed that the Type III biomass model is valid to one or two orders of magnitude, based on Earth's values. The goal, again, is to use the biomass estimate to argue for or against the plausibility of a biosignature gas based on Earth's biomass surface density values, not to make any predictions of quantitative values.

Bioindicators are defined as the end product of the chemical reactions of a biosignature gas.

Model caveats are related to the order-of-magnitude nature of the biomass estimates, the possible terracentricity of the biomass model estimates, and the lack of ecosystem context (see Seager et al. 2013, Sections 6.1– 6.3 for a detailed discussion). Here, we provide a summary overview.

The order-of-magnitude nature of the Type I biomass estimate derives from the dependency of the estimate on P_{m_e}, itself very sensitive to temperature. The possible terracentricity of our estimates is related to the use of P_{m_e}, which is derived from observations of terrestrial microorganisms, but we argue that the dependency is largely based on thermodynamics (Seager et al. 2013). The order-of-magnitude nature of the Type III biosignatures derives from the reliance on laboratory rates for microbial production rates; this is also possibly a terracentricity issue.

The lack of ecosystem context is a major limitation for the biomass estimate. An ecosystem contains not only the producers (i.e., the biomass estimate derived ultimately from the bioflux F_{source}) but also the consumers, whereas the biomass model

estimate considers only the producers. In this sense, the biomass estimate in Equation (4) is a minimum. We can fairly say that in the case of a very small or very large biomass estimate, the assessment of biosignature gas plausibility is valid: a small biomass estimate gives room for consumers even as a minimum biomass and a large biomass estimate as a minimum will remain large regardless of the consumers. For the intermediate case where a large but not unreasonable biomass is needed to generate a detectable biosignature, the decision of whether the gas is a plausible biosignature is more complicated and will depend on the planetary context: geochemistry, surface conditions, atmospheric composition, and other factors.

Again, we do not argue that the biosignature biomass model estimates are an accurate prediction of an extraterrestrial ecology. Rather, we emphasize that the goal of the biomass model estimates is the order-of-magnitude nature for a first-order assessment of the plausibility of a given biosignature gas candidate.

2.3. Detection Metric

We now describe our metric for a "detection" that leads to a required biosignature gas concentration. For now, detection has to be a theoretical exercise using synthetic data. We determine the required biosignature gas concentration based on a spectral feature detection with a signal-to-noise ratio (S/N) = 10. Specifically, we describe the S/N of the spectral feature as the difference between the flux in the absorption feature and the flux in the surrounding continuum (on either side of the feature), taking into account the uncertainties on the data:

$$\mathrm{S/N} = \frac{|F_{\mathrm{out}} - F_{\mathrm{in}}|}{\sqrt{\sigma_{F_{\mathrm{out}}}^2 + \sigma_{F_{\mathrm{in}}}^2}}, \quad (7)$$

where $F_{\mathrm{in}} \pm \sigma_{F_{\mathrm{in}}}$ is the flux density inside the absorption feature, $F_{\mathrm{out}} \pm \sigma_{F_{\mathrm{out}}}$ is the flux density in the surrounding continuum, and σ is the uncertainty on the measurement.

The uncertainties of the in-feature flux and continuum flux are calculated for limiting scenarios. For thermal emission, we consider a futuristic space telescope able to block out the light of the host star. The uncertainties of the in-feature flux and continuum flux are calculated for a limiting scenario: a 1.75 times Earth-sized planet orbiting a star[6] at 10 pc observed (via direct imaging) with a 6 m diameter telescope mirror operating within 50% of the shot noise limit and a quantum efficiency of 20%. The integration time is assumed to be 20 hr. We note that collecting area, observational integration time, and source distance are interchangeable depending on the time-dependent observational systematics. This telescope scenario is based on a TPF-I type telescope (Lawson et al. 2008).

For transit transmission spectra, we use the same equation as above but with the denominator replaced by the noise in the stellar flux (F_*), as in $\sqrt{(4\sigma_F^2)}$, because transmission observations measure the difference between the in-transit stellar flux and out-of-transit stellar flux. For transmission spectra, we consider a 6.5 m space telescope, having a quantum efficiency of 25% observing with a 50% photon noise limit, with integration time of 60 hr in-transit and 60 hr out of transit (assuming observing of multiple transits). Again, we note that collecting area, observational integration time, and source distance are interchangeable depending on the time-dependent observational systematics. This scenario is based on the *JWST*.

[6] Assuming perfect removal of starlight.

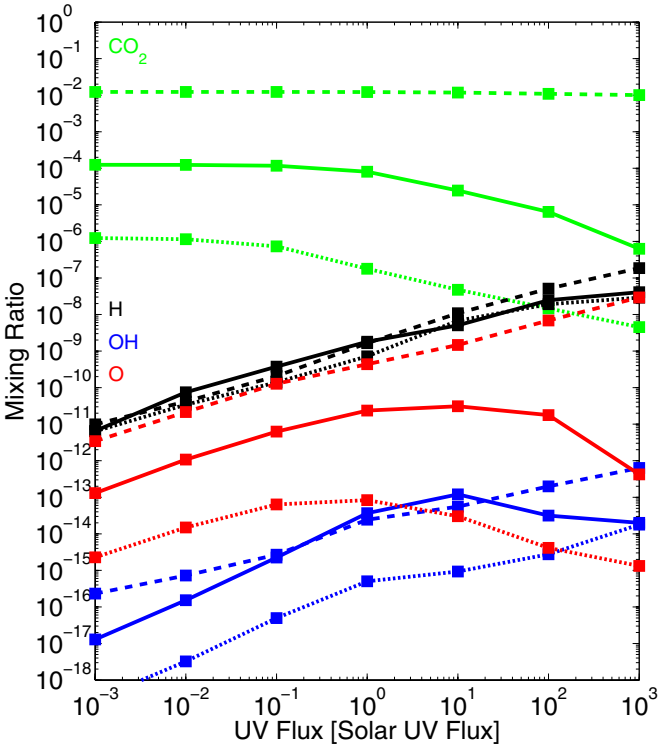

Figure 2. Mixing ratio dependence of the reactive species (H, OH, and O) on UV flux in a H_2-rich atmosphere with some CO_2. Different CO_2 levels are shown. The curves correspond to a CO_2 surface emission flux of Earth's volcanic emission rate (3×10^{15} m^2 s^{-1}; solid lines), a CO_2 emission rate 100 times higher than Earth's rate (dashed lines), and a CO_2 emission rate 100 times lower than Earth's rate (dotted lines). The planet has 10 $M_\oplus$ and 1.75 $R_\oplus$ and is in a 1.6 AU orbit around a Sun-like star (with UV adjusted). The fiducial atmosphere is 90% H_2 and 10% N_2 by volume, in a 1 bar atmosphere with a 290 K surface temperature. The main point is that the H concentration does not depend on the amount of CO_2 in the atmosphere, whereas the amount of O is critically controlled by the level of CO_2 in the atmosphere. Compared with H, OH is always a minor constituent in the atmosphere (by a few orders of magnitude). As the UV flux increases, more of the destructive, reactive species are generated. (A color version of this figure is available in the online journal.)

3. PHOTOCHEMISTRY RESULTS: H IS THE DOMINANT PHOTOCHEMICALLY PRODUCED REACTIVE SPECIES IN H_2-RICH ATMOSPHERES

In an H_2-rich terrestrial exoplanet atmosphere, atomic H is the largest sink for most atmospheric molecules including biosignature gases. This is in contrast with oxidizing atmospheres (atmospheres with substantial O_2 or CO_2 and H_2O and without H_2), where the OH radical (and in some cases O) plays the role of the dominant sink. We note that for H_2-rich atmospheres with high CO_2 levels, atomic O will be abundant (Figure 2) and for some molecules will dominate the removal chemistry.

To explain the high H concentration, we review the production of H, OH, and O in H_2-rich atmospheres. To qualitatively outline the main points, we use a simplified description of the main chemical pathways. This discussion serves for illustration only and is later backed up with a more detailed computational photochemistry model.

To derive atmospheric concentrations of a species [A], we take photochemical equilibrium,

$$\frac{d[A]}{dt} = P - [A]L = 0, \quad (8)$$

$$[A] = \frac{P}{L}, \tag{9}$$

where $[A]$ is the mixing ratio of species A and P and L are the production and loss rates, respectively, of species A. Below, the K terms are reaction constants and J is the photodestruction rate associated with a stated reaction.

We consider an H_2 atmosphere with some H_2O,

$$H_2O + h\nu \rightarrow H + OH \quad J, \tag{10}$$

$$OH + H_2 \rightarrow H_2O + H \quad K, \tag{11}$$

$$H + H + M \rightarrow H_2 + M \quad K_m. \tag{12}$$

Combining the above two equations, we have

$$[H] = \sqrt{\frac{K[OH][H_2]}{K_m[M]}} = \sqrt{\frac{J[H_2O]}{K_m}}, \tag{13}$$

and

$$[OH] = \frac{J[H_2O]}{K[H]}. \tag{14}$$

The simplified atmosphere reveals a number of relevant points. The first major point is that the role of OH in forming H from H_2 (Equation (11)) illustrates the importance of water vapor. Water is needed to form H in the first place, in this case.

The second major point is that the reason H can accumulate high concentrations is because the H + H + M reaction rate that removes the H atoms is relatively slow. The rates are

$$K = 2.8 \times 10^{-18} \exp(-1800.0/T) \quad [m^3\ s^{-1}], \tag{15}$$

$$K_m = 6.64 \times 10^{-39} (T/298.0)^{-1} \times N \quad [m^3\ s^{-1}], \tag{16}$$

$$J \simeq 10^{-6} \quad [s^{-1}], \tag{17}$$

where N is the number density of species M in units of molecules m^{-3}. The rates are from Sander et al. (2011).

The third major point is that in the H_2-rich atmosphere, the OH concentration is low because [OH] reacts with H_2 to recombine to H_2O.

H is produced by photodissociation of water vapor and not predominantly by the direct photodissociation of H_2. The reason is that the photons with high enough energy ($\lambda < 85$ nm; Mentall & Gentieu 1970) to photodissociate H_2 are not available. The high-energy photons that could dissociate H_2 directly are absorbed at the pressure levels of nanobars by H_2 itself and the photons that could penetrate down to pressure levels relevant to observations (0.1 mbar to 1 bar) are those that can dissociate water. Photodissociation of H_2O, in comparison, is caused by photons of lower energy ($\lambda \leqslant 240$ nm; Banks & Kockarts 1973), photons that can penetrate more deeply in the atmosphere than the ones that photodissociate H_2. We note that like other photochemical products, H is formed primarily above the mbar level, before all of the photodissociating stellar photons are absorbed.

The H concentration is dependent on the stellar UV levels and the presence of H_2O. Low-UV environments are favorable for biosignature build up, since the initial photolysis that starts the OH formation chain will be weaker. A similar situation is described for oxidized atmospheres in Segura et al. (2005).

We must be aware that for some molecules, in some situations, atomic O will be the dominant destructive species. There is no simple model (as in the above equations) but with our full simulation we find in atmospheres with high CO_2 that atomic O will abundant (see Figure 2). The key point is that reaction rates with O are faster than reaction rates with H for some molecules (see Table 1).

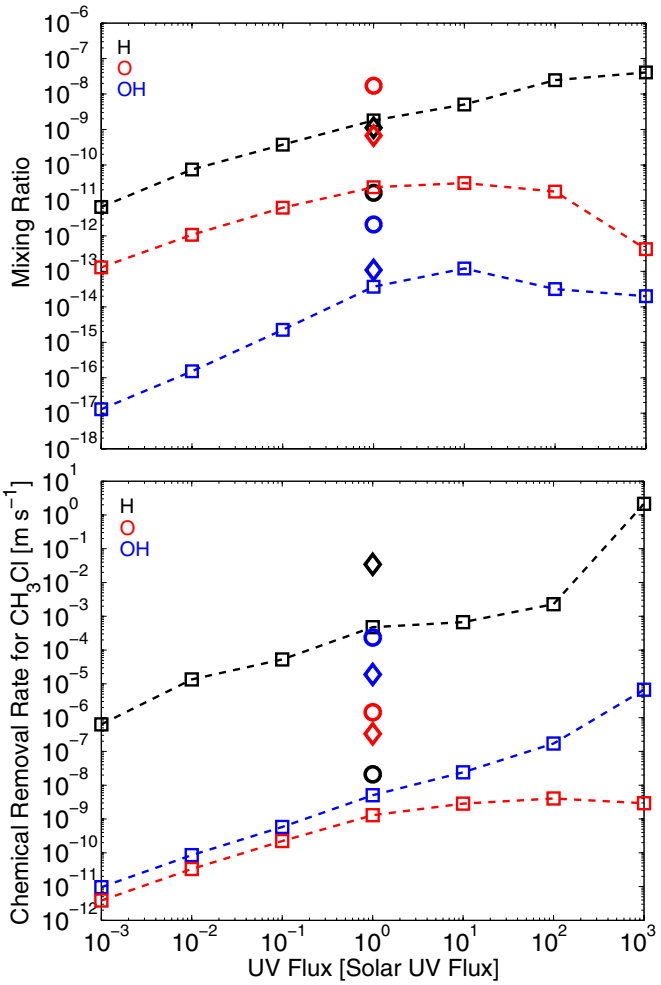

Figure 3. Destructive power of reactive species (H, OH, and O) in a reduced atmosphere. The atmosphere considered has 90% H_2 and 10% N_2 by volume, with CO_2, CH_4, SO_2, and H_2S emission from its surface, for a 1 bar atmosphere on a planet with 10 $M_\oplus$ and 1.75 $R_\oplus$. Shown for comparison are cases for an N_2-dominated atmosphere (diamonds) and Earth's current atmosphere (circles). Top panel: mixing ratios of H, OH, and O as a function of UV flux. The mixing ratio of H exceeds that of the other reactive species OH and O. Bottom panel: the column-integrated chemical removal rates as a result of reactions with H, O, and OH, for which we have used CH_3Cl as an example. The removal rates are scaled by the steady-state mixing ratio of CH_3Cl to have a dimension of velocity. This panel shows that removal by H is the dominant loss rate and that the loss rates scale approximately linearly with UV flux incident on the exoplanet atmosphere.

(A color version of this figure is available in the online journal.)

There is a very important point of comparison between the dominant reactive species, H in H_2-rich atmospheres and OH in oxidized atmospheres. The concentrations of H and OH in the two different types of atmospheres vary (see Figure 3 and Table 1, as well as more generally Table 4 in Hu et al. 2012). This can be understood qualitatively because OH is much more reactive than H. OH will react faster with any atmospheric component than H and so, for the same impinging stellar UV flux, OH will build up to a lower atmospheric concentration than H. The rate of removal of a biosignature gas by H or OH is a product of the concentration and the reactivity. OH, with a lower concentration but a greater reactivity, will remove a biosignature

Table 1
Reaction Rates with H, OH, and O of Select Type III Biosignature Gases

Reaction	A	n	E	$T = 270$ K	$T = 370$ K	$T = 470$ K
$DMS + H \rightarrow CH_3SH + CH_3$	4.81×10^{-18}	1.70	9.00	2.63×10^{-24}	2.11×10^{-22}	2.91×10^{-21}
$CH_3Cl + H \rightarrow CH_3 + HCl$	1.83×10^{-17}	0	19.29	1.97×10^{-24}	1.46×10^{-22}	1.92×10^{-21}
$CH_3Br + H \rightarrow CH_3 + HBr$	8.49×10^{-17}	0	24.44	1.59×10^{-21}	3.01×10^{-20}	1.63×10^{-19}
$CH_3I + H \rightarrow CH_3 + H_1$	2.74×10^{-17}	1.66	2.49	7.67×10^{-18}	1.75×10^{-17}	3.09×10^{-17}
$DMS + OH \rightarrow CH_3SCH_2 + H_2O$	1.13×10^{-17}	0	2.10	4.43×10^{-18}	5.71×10^{-18}	6.60×10^{-18}
$CH_3Cl + OH \rightarrow CH_2Cl + H_2O$	1.40×10^{-18}	1.60	8.65	2.54×10^{-20}	1.89×10^{-19}	3.17×10^{-19}
$CH_3Br + OH \rightarrow CH_2Br + H_2O$	2.08×10^{-19}	1.30	4.16	2.87×10^{-20}	7.13×10^{-20}	1.30×10^{-19}
$CH_3I + OH \rightarrow CH_2I + H_2O$	3.10×10^{-18}	0	9.31	4.90×10^{-20}	1.50×10^{-19}	2.86×10^{-19}
$DMS + O \rightarrow CH_3SO + CH_3$	1.30×10^{-17}	0	−3.40	5.91×10^{-17}	3.93×10^{-17}	3.10×10^{-17}
$CH_3Cl + O \rightarrow CH_2Cl + OH$	1.74×10^{-17}	0	28.68	1.77×10^{-23}	8.77×10^{-22}	8.26×10^{-21}
$CH_3Br + O \rightarrow CH_2Br + OH$	2.21×10^{-17}	0	30.76	1.77×10^{-23}	8.77×10^{-22}	8.26×10^{-21}
$CH_3I + O \rightarrow CH_3 + IO$	6.19×10^{-18}	0	-2.84	2.19×10^{-17}	1.56×10^{-17}	1.28×10^{-17}

Notes. Second-order reaction rates in units of m^3 molecule^{-1} s^{-1} are computed from the formula $k(T) = A(T/298)^n \exp(-E/RT)$, where T is the temperature in K and R is the gas constant (8.314472×10^{-3} kJ mole^{-1}). The reactions rate are compiled from the NIST Chemical Kinetics Database.

gas at a similar rate to H, which has a greater concentration but a lower reactivity. In other words, while the mechanism of chemistry clearance and the end products are different, the loss rates are fairly similar. For more details of the formation and destruction of the reactive species H, OH, and O in reduced and oxidized atmospheres, we refer the reader to Hu et al. (2012).

4. RESULTS: POTENTIAL AND UNLIKELY BIOSIGNATURE GASES

We now turn to describing the potential and unlikely biosignature gases in an H_2 atmosphere by their biosignature category. The biosignature categories developed in Seager et al. (2013) and summarized in Section 2.2 are an essential aide for calculations because of the common formation pathways that belong to each biosignature class.

We consider a planet with 10 $M_\oplus$, 1.75 $R_\oplus$, and an atmosphere with 90% H_2 and 10% N_2 by volume. The atmosphere scenario is the hydrogen-rich case among the exoplanet benchmark scenarios detailed in Hu et al. (2012) and we outline here the key specifics. The planet surface pressure is 1 bar and the planet surface temperature is 290 K. The temperature drops with increasing altitude according to an adiabatic lapse rate, until it reaches 160 K and is prescribed as a constant, as discussed above. The semi-major axis of the planets orbit is 1.4 AU if orbiting a Sun-like star and 0.037 AU if orbiting an M5V dwarf star; this is the consistent planet–star separation given the atmospheric composition and the required surface temperature. The eddy diffusion coefficients are scaled up by a factor of 6.3 from those measured in Earths atmosphere, in order to account for the difference in the mean molecular mass. Important minor gases considered are H_2O (evaporated from a liquid water ocean), CO_2 (about 100 ppm), and CH_4 and H_2S (emitted from surface). The deposition velocities of H_2 and CH_4 are assumed to be zero and the deposition velocity of CO is 10^{-10} m s^{-1}. The deposition velocities of oxidants, including O_2, O_3, H_2O_2, and sulfur species, are assumed to be the same values as on Earth. We refer the reader to Hu et al. (2012) for the rationale for these specifics and for the description of the carbon, oxygen, and sulfur chemistry in such an H_2-dominated atmosphere.

The amount of UV flux on the planet from the star is critical to destroying biosignature gases and so we consider the same planet orbiting three different stellar types. The first stellar type is a Sun-like star. The second stellar type is a weakly active 0.2 $R_\odot$ M5V dwarf star, with the extreme UV (EUV) taken as that expected for GJ 1214b (France et al. 2013). The third stellar type is a quiescent M star with no chromospheric radiation and only photospheric radiation, again a 0.2 $R_\odot$ M5V dwarf star (see Section 5.6). UV radiation received by the planet is scaled according to the semi-major axis and the stellar UV spectra are from the Air Mass Zero reference spectrum for the Sun-like star (http://rredc.nrel.gov/solar/spectra/am0/); the UV fluxes are from France et al. (2013) for the weakly active M dwarf star (using the values for GJ 1214b) and from simulated spectra of cool stars (Allard et al. 1997) for the UV-quiet M dwarf star (see Figure 1).

Whether or not a biosignature gas is detectable can be technique- and spectral-feature-dependent. The required atmospheric concentration depends on the strength of a given absorption feature and different techniques are sensitive to different wavelength ranges. For example, the thermal emission detection sensitivity follows the planetary thermal emission flux (approximately a blackbody peaking in the mid-infrared, mid-IR), whereas the transmission spectra sensitivity in the IR follows the thermal emission flux of the star (approximately a blackbody). An illustrative example is NH_3 with a strong absorption feature at 10.3–10.7 μm suitable for planetary thermal emission. For transmission, however, a weaker absorption feature at 2.8–3.2 μm is more easily detected than the 10 μm feature because of the overall photon fluxes of the star. For transmission spectra, we avoid consideration of Sun-like stars because the observational signal (the planet atmosphere-star area ratio) is too low (e.g., Kaltenegger & Traub 2009).

Biosignature gas results are summarized for thermal emission detectability (for Sun-like and M dwarf stars) in Table 2 and for transmission spectra detectability (for M dwarf stars only) in Table 3. Select promising biosignature gases are shown via their thermal emission spectra for a variety of atmospheres for intercomparison: CH_3Cl (Figure 4), DMS (Figure 5); N_2O (Figure 6), NH_3 (see Seager et al. 2013, Figure 2), and via their transmission spectra for H_2-dominated atmospheres (Figure 7).

4.1. Type I Biosignature Gases: Fully Reduced Forms

We start by focusing on the Type I biosignature gases, gases generated by reactions that extract energy from external, environmental redox gradients. The most likely Type I metabolic product in an H_2-rich atmosphere would be that in which

Table 2
Results for Thermal Emission Spectra

Molecule	Mixing Ratio (ppm)	Wave-length (μm)	Surf. Flux Sun-like (m^{-2} s^{-1})	Biomass Estimate (g m^{-2})	Surf. Flux Active M (m^{-2} s^{-1})	Biomass Estimate (g m^{-2})	Surf. Flux Quiet M (m^{-2} s^{-1})	Biomass Estimate (g m^{-2})	Dominant Removal Path
				Type I					
NH_3	0.10	10.3–10.8	2.4×10^{15}	4.0×10^{-4}	5.1×10^{14}	8.0×10^{-6}	8.2×10^{5}	9.5×10^{-6}	Photolysis
				Type III					
CH_3Cl	9.0	13.0–14.2	1.0×10^{17}	2.8×10^{3}	2.9×10^{15}	77	4.7×10^{11}	0.013	H
DMS	0.10	2.2–2.8	4.2×10^{19}	190	1.8×10^{19}	82	2.4×10^{13}	1.1×10^{-4}	O
CS_2	0.59	6.3–6.9	8.7×10^{17}	5.5×10^{7}	3.6×10^{17}	2.3×10^{7}	5.9×10^{11}	37	O
OCS	0.10	4.7–5.1	2.5×10^{15}	1.3×10^{5}	1.0×10^{14}	5.5×10^{3}	1.3×10^{10}	0.67	H
N_2O	0.38	7.5–9.0	3.8×10^{15}	...	5.4×10^{14}	...	1.3×10^{11}	...	Photolysis

Notes. Potential required biosignature gas concentrations, related required biosignature gas surface fluxes (in units of molecules m^{-2} s^{-1}), estimated biomass surface densities, and the dominant removal path or destructive species. Results are given for three cases: for a planet orbiting a Sun-like star, a weakly active M5V dwarf star (denoted "Active M"), and a quiescent M5V dwarf star (denoted "Quiet M"). The planet considered has 10 $M_\oplus$, 1.75 $R_\oplus$, an atmosphere with 90% H_2 and 10% N_2 by volume, a surface temperature of 290 K, and a surface pressure of 1 bar. Note that for compounds with a removal path dominated by O, the required surface flux sensitively depends on the CO_2 emission/deposition.

Table 3
Results for Transmission Spectra

Molecule	Mixing Ratio (ppm)	Wave-length (μm)	Surf. Flux Active M (m^{-2} s^{-1})	Biomass Estimate (g m^{-2})	Surf. Flux Quiet M (m^{-2} s^{-1})	Biomass Estimate (g m^{-2})	Dominant Removal Path
			Type I				
NH_3	11	2.8–3.2	5.5×10^{16}	1.1	8.8×10^{7}	1.8×10^{-9}	Photolysis
			Type III				
CH_3Cl	10	3.2–3.4	3.2×10^{15}	8.6×10^{2}	5.2×10^{11}	1.4×10^{-2}	H
DMS	0.32	3.1–3.6	5.8×10^{19}	2.6×10^{2}	7.8×10^{13}	3.6×10^{-4}	O
CS_2	0.38	6.4–6.9	2.3×10^{17}	1.5×10^{7}	3.8×10^{11}	24	O
OCS	1.8	4.7–5.1	1.9×10^{15}	9.9×10^{4}	2.3×10^{11}	12	H
N_2O	11	3.8–4.1	4.8×10^{15}	...	3.7×10^{12}	...	Photolysis

Notes. Potential required biosignature gas concentrations, related required biosignature gas surface fluxes (in units of molecules m^{-2} s^{-1}), estimated biomass surface densities, and the dominant removal path or destructive species. Results are given for two cases: a planet orbiting a weakly active M5V dwarf star (denoted "Active M") and a quiescent M5V dwarf star (denoted "Quiet M"). The planet considered has 10 $M_\oplus$, 1.75 $R_\oplus$, an atmosphere with 90% H_2 and 10% N_2 by volume, a surface temperature of 290 K, and a surface pressure of 1 bar. Note that a planet orbiting a Sun-like star is not considered for transmission spectra because the overall detection signal is too low because of the small ratio of planet atmosphere annulus area to star area. Note that for compounds with a removal path dominated by O, the required surface flux sensitively depends on the CO_2 emission/deposition.

non-hydrogen elements are in their most hydrogenated form.[7] In a reducing environment, life captures chemical energy by reducing environmental chemicals. In the presence of excess hydrogen, the most energy that life could extract from chemical potential energy gradients would be from converting elements from relatively oxidized compounds to their fully reduced form. An additional reason for focusing on Type I biosignature gas products that are in their most hydrogenated form is that they are likely long lived in an H_2-dominated atmosphere because molecules in their most hydrogenated form cannot undergo any further reactions with H.

4.1.1. Type I Biosignature Gas Overview

The most reduced form of the most abundant non-metal elements, C, N, O, P, S, H, Si, F, and Cl are CH_4, NH_3, H_2O, PH_3, H_2S, H_2, SiH_4, HCl, and HF. The most promising Type I biosignature gas is NH_3, which is further described below (Section 4.1.2). The other reduced molecules are unlikely biosignature gases for a variety of reasons. Some (PH_3, SiH_4) require energy input to make the reduced product from geologically available materials and so would not be produced by Type I biosignature gas reactions. Some are always present in their most reduced form and so life cannot reduce them further (HF, HCl). H_2S and CH_4 are not viable for the reasons discussed below, largely because geological and biologically sources cannot be discriminated between. In the case of H_2 and H_2O, they are naturally present in an H_2-dominated atmosphere at relevant potentially habitable planet temperatures.

As an aside about phosphine (PH_3), we note that trace amounts of phosphine are produced by some anaerobic ecologies on Earth (Glindemann et al. 2005). It is controversial whether the microorganisms in these environments are making PH_3 or whether the bacteria are making acid that is attacking environmental iron that contains traces of phosphide and this attack is making the phosphine gas (Roels & Verstraete 2001). Phosphine is a potential biosignature in other highly reduced

[7] Life might produce molecules with elements in intermediate redox states as life does on Earth. In an H_2 atmosphere, such molecules are likely to be photochemically hydrogenated.

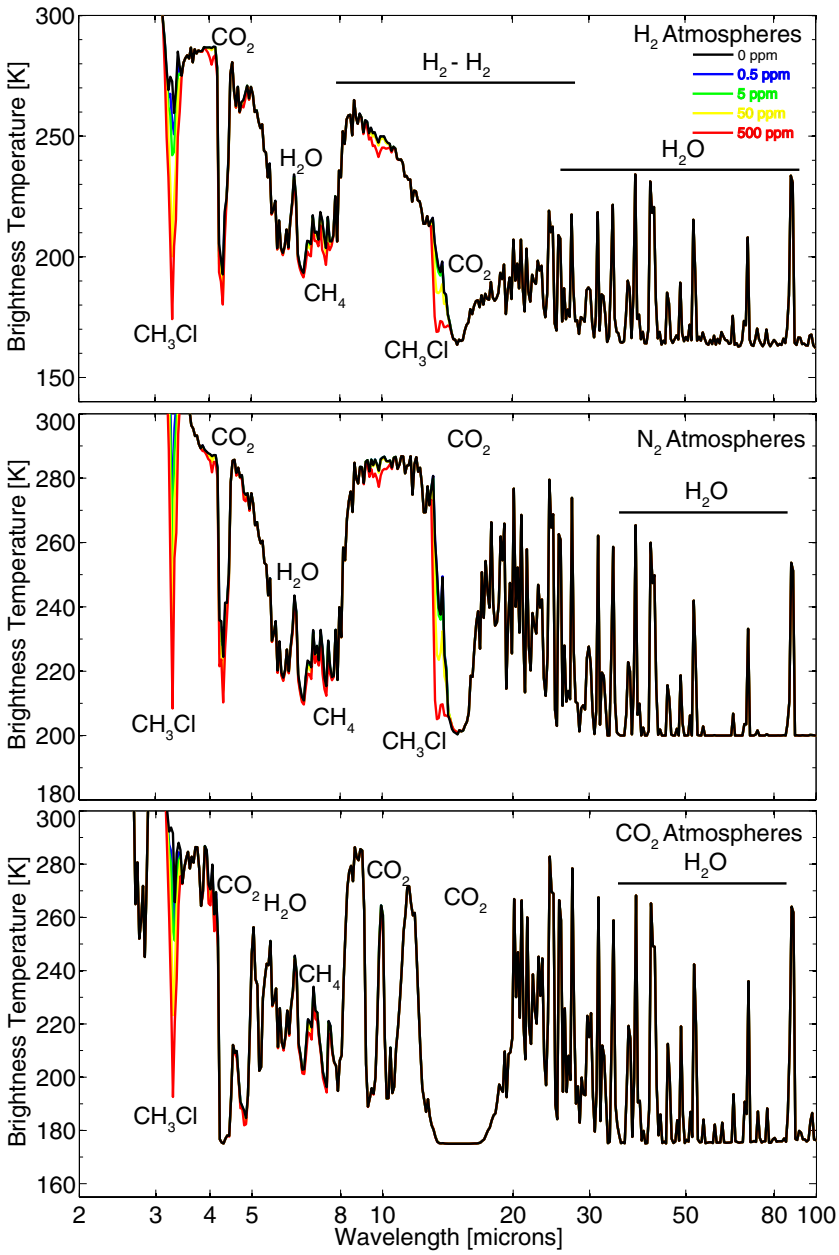

Figure 4. Theoretical IR thermal emission spectra of a super-Earth exoplanet with various levels of atmospheric CH_3Cl in a 1 bar atmosphere with a surface temperature of 290 K for a planet with 10 $M_\oplus$ and 1.75 $R_\oplus$. From top to bottom, the panels show the spectra of H_2-, N_2-, and CO_2-dominated atmospheres, respectively, and the detailed compositions of these reference atmospheres are described in Section 4 for the H_2-dominated planet and in Hu et al. (2012) for the N_2- and CO_2-dominated cases. We find that over 5 ppm of CH_3Cl is required for detection via thermal emission for the H_2-, N_2-, and CO_2-dominated atmospheres.

(A color version of this figure is available in the online journal.)

environments. Phosphine is reactive and thermodynamically disfavored over elemental phosphorus and hydrogen at the surface pressure and temperature of the Earth. Phosphine might be a Type I biosignature gas under conditions of very high H_2 pressure, which would favor the production of PH_3 over elemental phosphorus. Phosphine could be also be produced as a Type III biosignature gas, analogous to reactive signaling molecules such as NO or C_2H_4 on Earth.

4.1.2. NH_3 as the Strongest Candidate Biosignature Gas in an H_2 Atmosphere

NH_3 is the strongest candidate biosignature gas in a thin, H_2 atmosphere because, like O_2 in Earth's atmosphere, there is no plausible geological or photochemical mechanism for producing high concentrations on rocky planets with thin atmospheres (but cf. the false positive discussion below). NH_3 is readily photolyzed in the upper atmosphere to yield N_2 and is thermally broken down in volcanic gases at high temperatures. The triple bond of N_2 makes it extremely kinetically stable and so any N in the atmosphere ends up being trapped as N_2.

We have therefore proposed NH_3 as a biosignature gas in an H_2-rich atmosphere (Seager et al. 2013). NH_3 is a good biosignature gas candidate for any thin H_2-rich exoplanet atmosphere because of its short lifetime and lack of geological production sources. NH_3 as a biosignature gas is a new idea and one that is specific to a non-Earth-like planet. On Earth, NH_3 is not a useful biosignature gas because, as a highly valuable molecule for life that is produced in only small quantities,

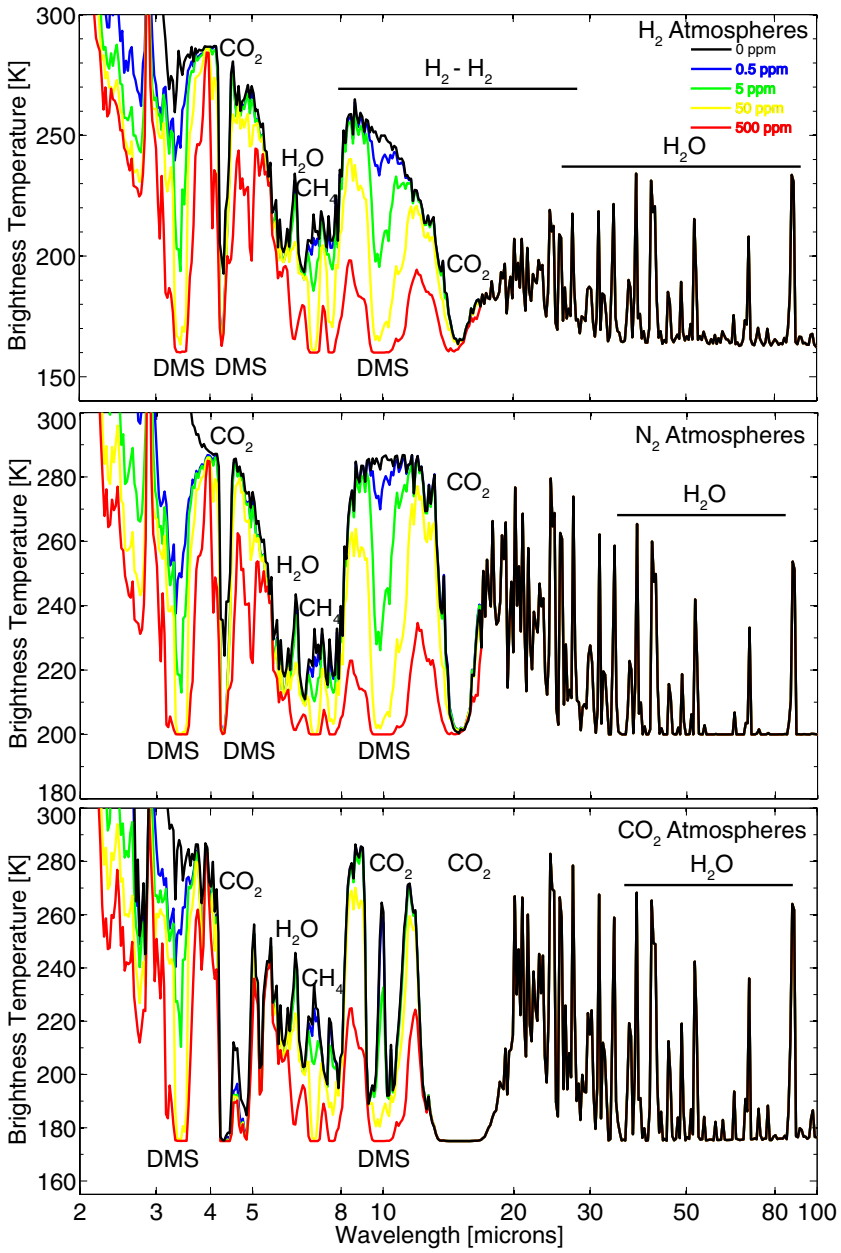

Figure 5. Theoretical IR thermal emission spectra of a super-Earth exoplanet with various levels of atmospheric DMS in a 1 bar atmosphere with a surface temperature of 290 K for a planet with 10 $M_\oplus$ and 1.75 $R_\oplus$. From top to bottom, the panels show the spectra of H_2-, N_2-, and CO_2-dominated atmospheres, respectively, and the detailed compositions of these reference atmospheres are described in Section 4 for the H_2-dominated planet and in Hu et al. (2012) for the N_2- and CO_2-dominated cases. We find that 0.1 ppm of DMS is required for future detection via thermal emission for the H_2-, N_2-, and CO_2-dominated atmospheres.

(A color version of this figure is available in the online journal.)

it is rapidly depleted by life and is unable to accumulate in the atmosphere. NH_3 is also a very poor biosignature gas on Earth because it is very soluble, so the trace amounts produced will stay dissolved in water and will not escape to the atmosphere.

The summary of the biosignature gas idea is that NH_3 would be produced from hydrogen and nitrogen, in an atmosphere rich in both:

$$3H_2 + N_2 \rightarrow 2NH_3. \quad (18)$$

This reaction is exothermic and could be used to capture energy. The industrial version of this reaction is called the Haber process for ammonia production at high temperatures; hence, we call such a planet a Cold Haber World. We proposed that in an H_2-rich atmosphere, life could find a way to catalyze the breaking of the N_2 triple bond and the H_2 bond to produce NH_3 and capture the energy released. In contrast, life on Earth solely fixes nitrogen in an energy-requiring process. Energy capture would yield an excess of NH_3 over that needed by life to build biomass, so the excess would accumulate in the atmosphere. Is a Cold Haber World possible? We believe yes, based on synthetic chemistry on Earth that can catalyze the breakage of each of the H_2 (Nishibayashi et al. 1998) and N_2 bonds (Yandulov & Schrock 2003; Schrock 2011) at Earth's surface pressure and temperature; what is not yet known is a catalytic system that can break both at once.

We showed in Seager et al. (2013) that for an Earth-sized, Earth-mass planet with a 1 bar atmosphere of 75% N_2 by volume and 25% H_2 by volume (including carbon species via a CO_2 emission flux), a potentially detectable NH_3 atmosphere

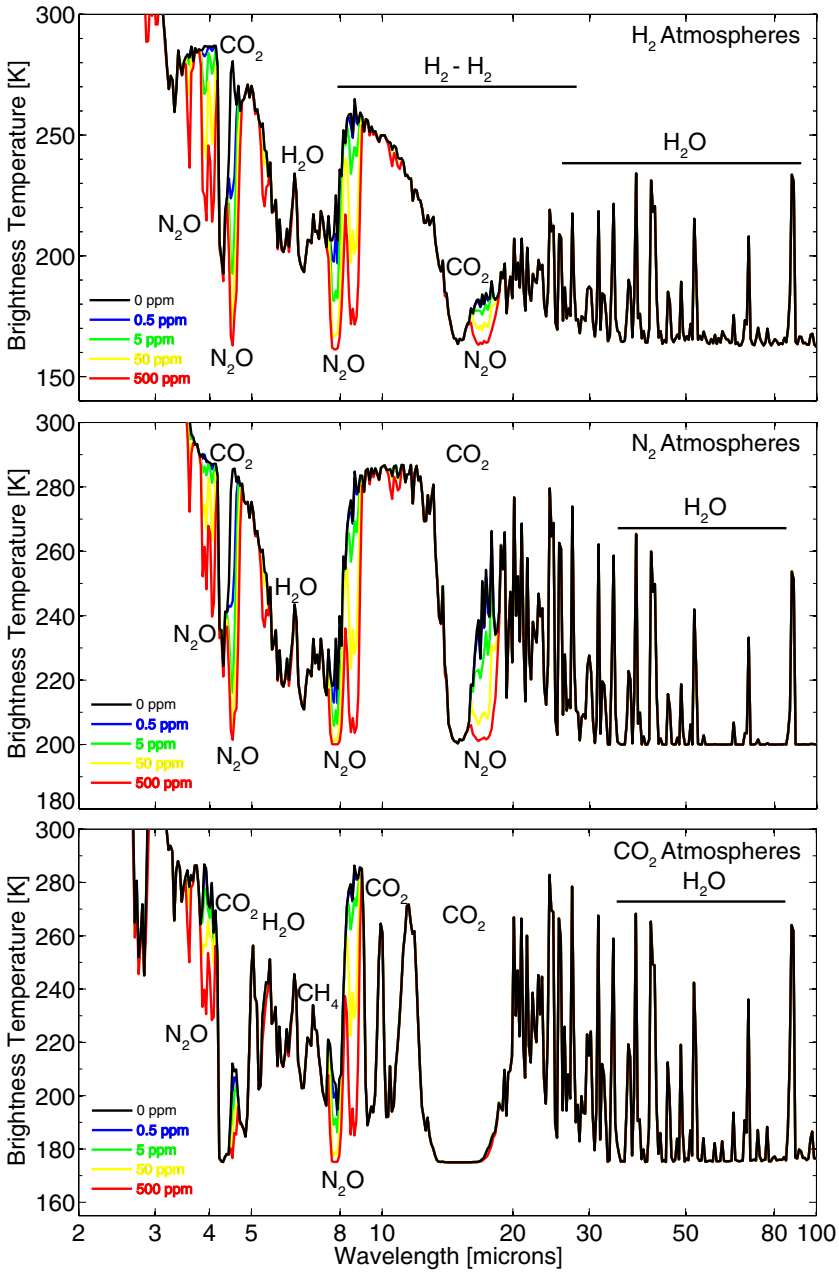

Figure 6. Theoretical IR thermal emission spectra of a super-Earth exoplanet with various levels of atmospheric N_2O in a 1 bar atmosphere with a surface temperature of 290 K for a planet with 10 $M_\oplus$ and 1.75 $R_\oplus$. From top to bottom, the panels show the spectra of H_2-, N_2-, and CO_2-dominated atmospheres, respectively, and the detailed compositions of these reference atmospheres are described in Section 4 for the H_2-dominated planet and in Hu et al. (2012) for the N_2- and CO_2-dominated cases. We find that about 0.4 ppm of N_2O is required for future detection via thermal emission for the H_2-, N_2-, and CO_2-dominated atmospheres.

(A color version of this figure is available in the online journal.)

concentration of 0.1 ppm is sustainable by a very reasonable biomass surface density of 9×10^{-2} g m^{-2}. This modest surface density corresponds to a layer less than one bacterial cell thick. For comparison, the phytoplankton that are the major contributor to Earth's oxygen atmosphere are present in Earth's oceans at around 10 g m^{-2}. For interest, we note that standard printer paper is between 80 and 100 g m^{-2}.

For an H_2-dominated atmosphere with 90% H_2 and 10% N_2 on a planet with 10 $M_\oplus$ and 1.75 $R_\oplus$ orbiting a Sun-like star, but all other parameters the same as the above, the viability of NH_3 as a biosignature gas in a thermal emission spectrum still holds based on a physically reasonable biomass surface density. We now describe the estimate for the biomass surface density using the Type I biomass equation (Equation (4)). We use the NH_3 source flux of 2.4×10^{15} molecule m^{-2} s^{-1} (see Table 2). To compute ΔG, we used $T = 290$ K and reactant and product concentrations at the surface in terms of partial pressures of $N_2 = 0.1$, $H_2 = 0.9$, and $NH_3 = 1.4 \times 10^{-7}$, giving $\Delta G = 85.6$ kJ mole^{-1}. With $P_{m_e} = 7.0 \times 10^{-6}$ kJ g^{-1} s^{-1}, we find a biomass surface density of 4.9×10^{-2} g m^{-2}. Based on this reasonable biomass surface density, we therefore consider the NH_3 production flux to be viable in our Haber World scenario. The global annual biogenic NH_3 surface emission in the Haber World would be about 1100 Tg yr^{-1}. This is much higher than Earth's natural NH_3 emission at 10 Tg yr^{-1} (Seinfeld & Pandis 2000). Comparing NH_3 production on the Haber World and on

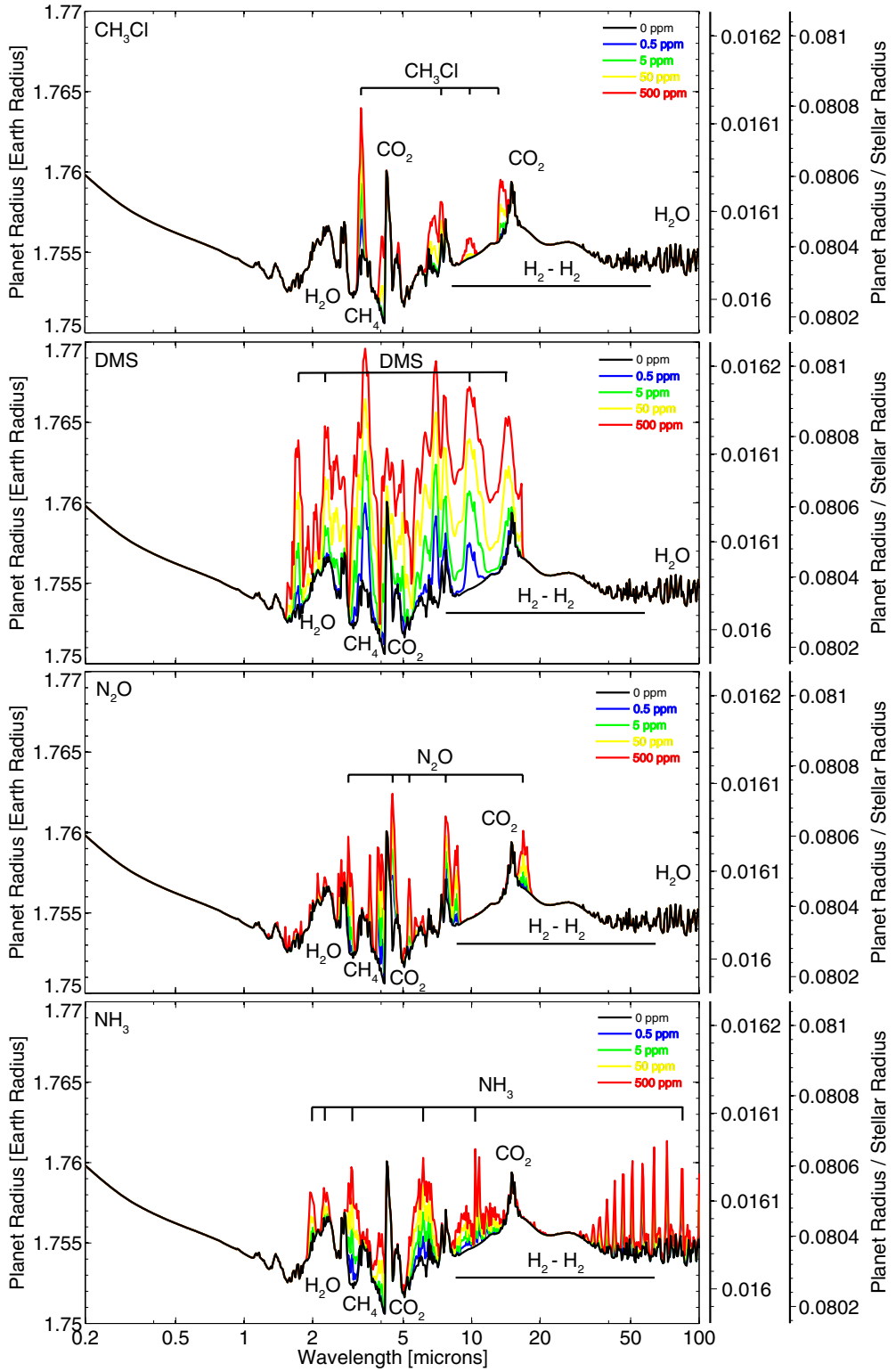

Figure 7. Theoretical transmission spectra for potential biosignature gases in a 10 $M_\oplus$, 1.75 $R_\oplus$ planet with a 1 bar atmosphere composed of 90% H_2 and 10% N_2, with a surface temperature of 290 K. Potential biosignature gases, including CH_3Cl, DMS, N_2O, and NH_3, have spectral features in IR wavelengths from 1 to 10 μm, making these gases detectable at various atmospheric mixing ratios (see Table 3).

(A color version of this figure is available in the online journal.)

Earth, however, is not valid. We are postulating that production of NH_3 on the Haber World is a major source of metabolic energy for life. A better emission rate comparison is to compare the biosignature gas O_2 from Earth's principal energy metabolism, photosynthesis. The Earth's global oxygen flux is 200 times larger than the Haber World's NH_3 surface emission, at about 2×10^5 Tg yr^{-1} (Friend et al. 2009).

Turning to a weakly active M5V dwarf star, for the same fiducial planet, the NH_3 surface flux required to sustain a detectable level of atmospheric NH_3 in a thermal emission

spectrum is 5.1×10^{14} molecule m^{-2} s^{-1} (see Table 2). This value is about five times lower than the Sun-like star example above and therefore converts into a biomass estimate about five times smaller than the Sun-like star example above, or about 1×10^{-2} g m^{-2}, due to the linear scaling of the problem. For a transmission spectrum measurement for the same planet orbiting the same weakly active M dwarf star, the optimal wavelength range for detection is 2.8–3.2 μm, the required concentration is 11 ppm, and the required surface source flux is 5.5×10^{16} molecule m^{-2} s^{-1}, resulting in a surface biomass of 1 g m^2. For this particular example, NH_3 in transmission versus thermal emission, it is more difficult to detect NH_3 and hence a higher biomass is actually required for the same hypothetical type of life.

We emphasize that the NH_3 biosignature gas concept is not changed for a planet with a massive (yet still "thin") atmosphere with high surface pressure. As long as the surface conditions are suitable for liquid water, NH_3 will not be created by uncatalyzed chemical reactions.

NH_3 is not immune to false positives. Although a rocky planet with a thin H_2-dominated atmosphere is unlikely to have an NH_3 false positive, the challenge is in identifying the planetary (and stellar) characteristics. We describe three scenarios that could lead to the nonbiological production of NH_3.

A rocky world with a hot surface of ~820 K could generate NH_3 by the conventional Haber process if there is surface iron. Such a hot surface temperature could presumably be ruled out from other observations.

A second scenario where NH_3 is naturally occurring is in the atmospheres of gas giant planets or the so-called mini-Neptunes. The deep atmosphere may reach conditions where NH_3 can be formed kinetically at the extremely high pressures necessary for NH_3 formation to be possible thermodynamically. On Jupiter, for example, the $H_2 + N_2 \rightarrow NH_3$ reaction becomes significant in comparison with vertical transport at about 1500 K and 1400 bar (Prinn & Olaguer 1981). The only way we can discriminate between planets with a massive envelope and a rocky planet with a thin atmosphere where the pressures for the thermodynamic formation of NH_3 are not reached is with high-resolution spectra to assess the surface pressure (Benneke & Seager 2012, 2013).

A third scenario for an NH_3 false positive is for planets with outgassed NH_3 during evolution. The importance of ammonia for the atmospheric evolution of Titan relates to primordial ammonia that accreted with the ices of the moon and has not subsequently been broken down either by internal heat (likely on a rocky planet) or by external UV photolysis (which will rapidly break down any NH3 in the atmosphere; Shin et al. 2012). In this case, ammonia is therefore present as ice in the interior. This would be a challenging case to ascertain and illustrates how an assignment of any gas as a biosignature gas candidate has to be given a detailed probabilistic assessment based on what we know about the relevant planet.

For any case, for a quiescent M star with no chromospheric UV emission—hence a planet with little to no destructive UV flux—NH_3 can easily accumulate in the planet atmosphere and act as a significant false positive. NH_3 is destroyed by photolysis and is very sensitive to the amount of UV radiation.

4.1.3. CH_4 and H_2S as Unlikely Biosignature Gases

CH_4 has been described at length as a possible biosignature gas on early Earth and on exoplanets with oxidized atmospheres (e.g., Hitchcock & Lovelock 1967; Des Marais et al. 2002). This is despite the risk of a geologically derived false positive, because it is believed that in an oxidized environment geological production of CH_4 will be small, and so if enough CH_4 is produced it may be attributed to life. This is the case on Earth where at least 99% of the atmospheric CH_4 derives directly from life or from industrial destruction of fossil hydrocarbons formed from past life (Wang et al. 2004). However, the 1775 ppb concentration of CH_4 in Earth's atmosphere (Solomon et al. 2007) is not enough to be detected remotely with envisioned space telescope capabilities.

CH_4 is a poor biosignature gas in an H_2-rich atmosphere because it is both produced volcancially and is an end product of CO_2 photochemistry in the atmosphere. Terrestrial volcanic emission rates of CH_4 and CO_2 would lead to substantial buildup of CH_4 in H_2-dominated atmospheres. Even small amounts of outgassed CO_2 will lead to an accumulation of CH_4 in the atmosphere because CH_4 has a very long lifetime in an H_2-rich atmosphere and CH_4 would be produced by

$$4H_2 + CO_2 \rightarrow CH_4 + 2H_2O. \quad (19)$$

More specifically, considering Earth's volcanic emission rates of CH_4 and CO_2, and with deposition velocities of 10^{-6} m s^{-1} for CO_2 and 0 m^{-2} s^{-1} for CH_4, CH_4 will accumulate up to ~10 ppm in a 1 bar 90% H_2 and 10% N_2 atmosphere with a temperature profile similar to that of the Earth (Hu et al. 2012). Even in the case of no surface CH_4 emission, CO_2 emission into the same atmosphere would lead to the atmospheric production and accumulation of CH_4 up to 5 ppm. This example is intended to show that the false positive risk of CH_4 is so high in an H_2-dominated atmosphere as to make CH_4 an implausible biosignature gas.

H_2S is even more unfavorable than CH_4 as a biosignature gas in an H_2-rich atmosphere because of the same geological false positive issues as with carbon gases. An added problem is the generation of aerosols that may blanket any spectral features and the fact that the H_2S spectral features are heavily contaminated by atmospheric water vapor, making them potentially difficult to detect (Hu et al. 2013).

4.2. Type II Biosignature Gases: No Viable Biosignature Gases

Type II biosignature gases are those produced by metabolic reactions for biomass building. Biomass building on Earth primarily occurs by photosynthesis, which has the dual goal of harvesting light energy to use for metabolism and also capturing carbon for biomass building.

We have not identified any useful biosignature gases of Type II in an H_2-rich, 1 bar atmosphere. Photosynthesis in a reduced environment such as an H_2-dominated atmosphere would generate reduced by-product gases, which are not useful as biosignature gases because those species are already expected to be present in their most reduced forms in the H_2-dominated atmosphere.

The concept of photosynthesis on a planet with an H_2-dominated atmosphere is nonetheless worth some discussion,[8] starting with a brief review of photosynthesis in the familiar Earth environment. Photosynthesis must convert carbon from its environmental form, which is the form that is most thermodynamically stable at surface temperatures and pressures,

[8] See the AbSciCon 2008 abstract by N. Sleep http://online.liebertpub.com/doi/pdf/10.1089/ast.2008.1246, and Pierrehumbert & Gaidos (2011) for a discussion of photosynthetic active radiation that reaches the surface under thick H_2 atmospheres.

into biomass. The biomass is of an intermediate redox state (Bains & Seager 2012). The key point therefore is that in an oxidized environment like that of the Earth, photosynthesis must reduce oxidized carbon (CO_2) and will generate an oxidized by-product. On Earth, environmental carbon is captured in photosynthesis, producing O_2 as a by-product:

$$H_2O + CO_2 \rightarrow CH_2O + O_2. \quad (20)$$

Here, CH_2O represents biomass.

Photosynthesis, by definition, will have the same goal in an H_2-rich environment as in an oxidized environment: to harvest light energy and build carbon-based biomass. Because CH_4 is the most thermodynamically stable gaseous form of carbon in this environment, photosynthesis would oxidize the carbon in CH_4 and produce a reduced by-product. The lowest energy route is to directly split the CH_4 as

$$CH_4 + H_2O + X \rightarrow CH_2O + XH, \quad (21)$$

where X is an atom that is oxidized in the environment and has been reduced to XH, consuming energy in the process, and CH_2O again represents biomass. (We note that the oxidation state of the oxygen is not changed in this process, unlike oxygenic photosynthesis on Earth, so formally this is not splitting water even though water is involved.)

The null result for photosynthetic biosignatures in an H_2-dominated atmosphere is based on the point that most nonmetals (C, O, S, the halogens) are likely to be in their most reduced state already on the surface of this world and so cannot play the role of X in the photosynthesis process described above.

One exception might have been hydrogen, which is oxidized in water and methane and so a possible photosynthetic reaction is

$$CH_4 + H_2O \rightarrow CH_2O + 2H_2, \quad (22)$$

but again H_2 is not a useful biosignature gas because it is already present in the H_2-dominated atmosphere.

For completeness, we describe some other unlikely but interesting possibilities for X and XH. Silicon, phosphorus, and boron are likely to be present as the oxidized minerals silicates, phosphates, and borates, respectively, but using these as a sink for the electrons in photosynthesis, for example in the reaction with silica to generate silane,

$$CH_4 + \frac{1}{2}SiO_2 \rightarrow CH_2O + \frac{1}{2}SiH_4, \quad (23)$$

requires more energy than the reaction in Equation (22) under a range of conditions and so would represent a very inefficient way of generating biomass.

Reduction of a metal with a positive electrochemical potential would be more energetically efficient, as for example in the reduction of copper oxide to copper:

$$CH_4 + 2Cu(O) \rightarrow CH_2O + 2Cu + H_2O, \quad (24)$$

but this reduction produces no volatile product and is dependent on a supply of oxidized metal. (There are clear parallels with anoxygenic photosynthesis on Earth for this type of reaction.) In contrast, the reaction in Equation (22) is limited only by the supply of methane, as life in water is not limited by the chemical availability of water. In summary, photosynthesis in the reducing environment will either generate H_2, which will not be detectable in a hydrogen-dominated atmosphere, or will produce non-volatile products, i.e., products not in gas form, which, by definition, will not be detectable as atmospheric gases.

4.3. Type III Biosignature Gases are the Most Viable in Low-UV Environments

Life produces many molecules for reasons that are not related to the generation of energy, which we refer to as Type III biosignature gases. The gases are produced for reasons such as stress, signaling, and other physiological functions, and some of these have already been discussed quantitatively in detail as biosignature gases in oxidized atmospheres, (e.g., CH_3Cl (Segura et al. 2005) and DMS and other sulfur compounds (Domagal-Goldman et al. 2011)).

The fate of Type III biosignature gas molecules depends on the level of relevant reactive species in the atmosphere and hence on stellar UV flux. In low-UV environments, some Type III gases can accumulate to detectable levels. In the relatively high-UV environments of Sun-like stars, many Type III gases could be rapidly driven to their most hydrogenated form in an H_2-rich atmosphere. In some cases, they will not accumulate to detectable levels unless we assume unrealistic production rates. In these extreme cases in a high-UV environment, we would only be able to infer the presence of the biosignature gas by detecting the end product of photochemical attack, which we call a bioindicator. Only in a few cases might bioindicators be useful, because many are not spectroscopically active (and hence not detectable) and others are indistinguishable from geological cases as well (e.g., DMS will end up as CH_4 and H_2S; N_2O will end up as N_2 and H_2O.)

We now show that Type III biosignature gas survival and hence plausibility depends highly on the UV flux level of the host star. We consider the three fiducial stellar types that differ in UV radiation levels: a Sun-like star, a weakly active M5V dwarf star, and a quiescent M5V dwarf star (Figure 1). We consider the same model planet as above, a 10 $M_\oplus$, 1.75 $R_\oplus$ planet with an atmosphere with 90% H_2 and 10% N_2 by volume, with a surface temperature of 290 K and a surface pressure of 1 bar. Results for the cases we modeled are listed for thermal emission spectra in Table 2 and for transmission spectra in Table 3.

Our first example of a Type III biosignature gas is methyl chloride (CH_3Cl). CH_3Cl is produced in trace amounts by many microorganisms on Earth. The detectability of CH_3Cl in Earth-like atmospheres in the low-UV environment of UV-quiet M stars has already been studied by Segura et al. (2005) and later as a potential biosignature gas in more generalized oxidized atmospheres by Seager et al. (2013).

Here, for the first time, we study CH_3Cl as a potential biosignature gas in a thin H_2-rich atmosphere. For this, we go beyond previous work not only by considering an H_2 atmosphere but also by using our biomass estimate framework so as not to be constrained by terrestrial bioflux production rates. We now show why CH_3Cl is a potential biosignature gas in H_2-rich atmospheres in low-UV environments—because the amount of biomass needed to generate a detectable concentration of CH_3Cl is physically plausible. We use our biomass estimate framework (Section 2.2 and Seager et al. 2013).

Considering the thermal emission spectrum for our fiducial planet with a 1 bar atmosphere of 90% H_2 and 10% N_2, a spectral signature of 9 ppm is required for spectral detection using our detection metric. This statement is for a spectral band feature in absorption at 13.0–14.2 μm (see Figure 4); this is the band accessible in an H_2 atmosphere, weaker than the 6.6–7.6 μm band that would be masked by H_2–H_2 collision-induced absorption. In order to sustain an atmospheric concentration of 9 ppm of CH_3Cl on our model planet in

the habitable zone for a Sun-like star, a weakly active M5V dwarf star, and a UV-quiet M5V dwarf star, the surface bioflux production rate would need to be 1.0×10^{17} molecule m^{-2} s^{-1} (1.7×10^{-7} mole m^{-2} s^{-1}), 2.9×10^{15} molecule m^{-2} s^{-1} (4.8×10^{-9} mole m^{-2} s^{-1}), and 4.7×10^{11} molecule m^{-2} s^{-1} (7.8×10^{-13} mole m^{-2} s^{-1}), respectively. Estimating the biomass with Equation (6) and with the lab rate at 6.17×10^{-11} mole g^{-1} s^{-1} (see Seager et al. 2013), the biomass surface density would need to be about 3000 g m^{-2}, 80 g m^{-2}, and 0.001 g m^{-2} for each stellar type, respectively. A globally averaged density of 3000 g m^{-2} is likely too high; one of 80 g m^{-2} is high but not impossible, according to terrestrial biodensities (see Seager et al. 2013).

The results show that CH_3Cl is a more viable biosignature gas in low-UV environments compared with high-UV environments. We emphasize that although our estimates of biomass surface density for Type III biosignature production are approximate, the resulting trend is robust.

For a spectral detection in transmission for our fiducial Earth transiting an M5V star, the required concentration is about 10 ppm in the wavelength range 3.2–3.4 μm. The surface bioflux and biomass estimates for a weakly active and quiet star, respectively, are 3.2×10^{15} molecule m^{-2} s^{-1} and 900 g m^{-2} and 5.2×10^{11} molecule m^{-2} s^{-1} and 0.001 g m^{-2}. The required biomass surface density for the weakly active M star is higher than the average surface biomass in Earth's oceans and the biomass surface density for the quiet M5V dwarf star is much lower than that of the Earth and is very plausible, again emphasizing the trend that low-UV radiation environments are more favorable for Type III biosignature gas accumulation.

The different values for the biosignature gas surface flux and the biomass estimates for transmission spectra compared with thermal emission spectra are in general due to longer atmospheric pathlengths and/or different favorable wavelengths (depending on the molecule of interest).

The fate of CH_3Cl in its destruction by H is to end up in its fully hydrogenated form, HCl, with the overall reaction as given by

$$CH_3Cl + H_2 \rightarrow CH_4 + HCl. \quad (25)$$

HCl could be a bioindicator. The HCl molecule is stable against further photochemistry because if it is photolyzed, the Cl atoms generated will be predominately react with H to re-form HCl. HCl would not be expected to be present in significant levels at atmospheric altitudes for spectral detection without life taking non-volatile forms of Cl and putting them into the atmosphere, because all geological sources are non-volatile chlorides (such as NaCl) and any HCl that is volcanically released would be efficiently rained out of the troposphere. The limiting problem is that the HCl spectral features are too weak to be detectable and are likely to be contaminated by CH_4 in the 3–4 μm range.

As a second Type III biosignature gas example, we consider DMS. DMS has been studied before in oxidizing atmospheres by Domagal-Goldman et al. (2011), who concluded that DMS itself is not a potentially detectable biosignature gas in oxidized atmospheres under Sun-like UV radiation conditions, but one of its photolytic breakdown products, ethane, is detectable (we call this a "bioindicator" gas). Using the same atmosphere and framework as the above CH_3Cl example, we find a mixing ratio required for detection of 0.1 ppm in the 2.2–2.8 μm band (see Figure 5) for thermal emission spectra. Via photochemistry, this mixing ratio corresponds to a surface flux in our fiducial H_2-dominated atmosphere for a Sun-like star, a weakly active M5V dwarf star, and a quiet M5V dwarf star of 4.2×10^{19} molecules m^{-2} s^{-1} (6.9×10^{-5} moles m^{-2} s^{-1}), 1.8×10^{19} molecules m^{-2} s^{-1} (3.0×10^{-5} moles m^{-2} s^{-1}), and 2.4×10^{13} molecules m^{-2} s^{-1} (4.1×10^{-11} moles m^{-2} s^{-1}), respectively. Using a DMS lab production rate of 3.64×10^{-7} moles g^{-1} s^{-1} (Seager et al. 2013), we come up with an implied biomass surface density estimate for the three star types of about 200 g m^{-2}, 100 g m^{-2}, and 10^{-4} g m^{-2}, respectively. The first two values are high, but physically plausible compared with Earth's biomass surface density ranges. For transmission spectra, the numbers are about a factor of two higher for the weakly active and quiet M5V dwarf star (see Figure 7 and Table 3).

The DMS results show again that the lowest UV environment is the most favorable. There are two other relevant points related to DMS appearing to be a favorable biosignature gas in each of the three UV radiation environments studied. The first point is that gases destroyed by reactions with O (as opposed to gases destroyed by reactions with H) show a similar surface flux requirement between the Sun-like and weakly active M dwarf star. This is because the release of O from CO_2 photolysis is largely driven by Lyman α emission, which is similar at the habitable zones for the Sun-like and weakly active M dwarf stars used in this study (Figure 1).

The second point is that the high R_{lab} values used for DMS, and hence the low biomass surface density estimates, are a result of the biology of DMS production. On Earth, DMS is the waste product of consumption of Dimethylsulfoniopropionate (DMSP) by marine organisms consuming marine plankton. DMSP is accumulated in large amounts by some marine species. Thus, organisms that generate DMS do not have to invest their own resources to make DMS and so are not limited to how much they can make. Maximal production rates are therefore very high. This is discussed further in Seager et al. (2013).

In terms of a bioindicator, DMS will react with H_2 to generate CH_4 and H_2S. Neither is a useful bioindicator as CH_4 and H_2S are expected to be present in the atmosphere naturally. This is in contrast with oxidized atmospheres, where ethane may be a bioindicator gas, as expected for the end product of DMS photodestruction by the combination of methyl radicals generated from the attack of O on DMS (Domagal-Goldman et al. 2011).

As a third and fourth Type III biosignature gas example, we used CS_2 and OCS. For these two gases, we find the same trend as the other Type III biosignature gases: in a low-UV environment, the biosignature gases can accumulate (see Tables 2 and 3). The biomass estimates (as a plausibility check) are too high for the Sun-like and weakly active M dwarf stellar environments to be plausible compared with terrestrial biomass surface density values. OCS in the UV environment of a weakly active M dwarf star may be an exception with an estimate at the upper limit of plausibility.

As a fifth example, we describe N_2O. On Earth, N_2O is a Type I biosignature gas produced by nitrifying bacteria. N_2O is not likely to be produced in a thin H_2-rich atmosphere because there is unlikely to be much nitrate available. Here, we explain further. N_2O has been suggested as a biosignature gas in Earths atmosphere (Segura et al. 2005). N_2O is a Type I biosignature gas formed by two processes on Earth—the oxidation of ammonia by atmospheric oxygen and the reduction of nitrate in anoxic environments:

$$2NH_3 + 2O_2 \rightarrow N_2O + 3H_2O, \quad (26)$$

$$NO_3^- + H \rightarrow N_2O + H_2O. \quad (27)$$

Analogous reactions on a hydrogen-dominated world would be the reduction of nitrate by atmospheric hydrogen:

$$NO_3^- + H_2 \rightarrow N_2O + H_2O + OH^- \quad (28)$$

or the oxidation of ammonia by a geologically derived oxidant.

Nitrate is formed on Earth by the oxidation of NO generated by lightning in Earth's oxygen-rich atmosphere or by biological processes—neither are likely in an H_2-rich environment, so it is not clear whether nitrate reduction is a useful energy source in a world with an atmosphere rich in H_2. Ammonia oxidation requires a strong oxidizing agent, which again is likely to be missing from the environment.

N_2O as a Type I biosignature gas therefore seems unlikely, although not impossible, from very rare environments in which there are oxidized nitrogen species generated geochemically.

N_2O, however, could be a Type III biosignature gas as NO is for some organisms on Earth. We have calculated the surface fluxes for a detectable amount of N_2O in a thin, H_2-dominated atmosphere and find relatively low required surface fluxes. The reason is that N_2O is destroyed by photodissociation at a slower rate than by reaction with H. N_2O may therefore be a plausible biosignature gas candidate, even in an atmosphere subject to strong UV radiation (see Figures 6 and 7 and Tables 2 and 3). A biomass estimate (as a plausibility check) is not possible for N_2O, as it is only known as a Type I biosignature on Earth (and so therefore Type III R_{lab} rates are not available).

5. DISCUSSION

5.1. What Constitutes an H_2-dominated Atmosphere?

We have calculated biosignature gas accumulation in an atmosphere with 90% H_2 and 10% N_2 by volume. A super-Earth exoplanet atmosphere can have many other gas species. The concentration of the major destructive species (H, O, and OH) will depend on the amounts of these other gas species.

As an example, we explore the changing effect of the reactive species in an H_2-dominated atmosphere for different UV flux levels, based on the surface flux levels of CO_2 (Figure 2). A few key points are as follows. The H abundance is almost not affected by the CO_2 mixing ratios ranging from 10^{-8} to 10^{-2}. The O abundance depends on both CO_2 and UV levels, such that both a high CO_2 level and a high-UV flux lead to high atmospheric O. Only in extreme cases (e.g., H_2-dominated atmospheres with $>1\%$ CO_2, shown by dashed lines) is the abundance of O very close to the abundance of H. The OH abundance depends on a complex source-sink network, ultimately driven by H_2O and CO_2 photolysis. Notably, the amount of H is always at least four orders of magnitude larger than the amount of OH.

The effect of changing the H_2 mixing ratio and the addition and variation of other active gases on the H concentration will need to be considered in a case-by-case basis as they will react not only with H and OH but also with other gas species.

5.2. Can Super-Earths Retain H_2-dominated Atmospheres?

Whether or not a super-Earth planet can retain H_2 stably from atmospheric escape is not known. Although many models and studies for exoplanet atmospheric escape exist (see, e.g., Lammer et al. 2012 and references therein), the permanent limitation is that there are too many unknowns to provide a definitive and quantitative statement on which planets will retain H_2. One of the challenges is the unknown history and present state of the host star's EUV flux. Another major challenge is defining the mechanism for atmospheric escape for a given exoplanet, for example whether or not the regime of rapid hydrodynamic escape was reached in a planet's history or which non-thermal mechanism, if any was dominant (see Table 4.1, and references therein in Seager 2010). With an unknown initial atmospheric reservoir and an unknown present atmospheric composition, the regime and type of atmospheric escape is difficult to impossible to identify.

Some super-Earths will have been formed with atmospheres with H_2, based on both theoretical and observational evidence. Theoretically, planetary building blocks contain water-rich minerals that can release H (Elkins-Tanton & Seager 2008; Schaefer & Fegley 2010). Observationally, the large number and variety in radii of *Kepler* mini-Neptunes imply that these objects have an H or an H/He envelope to explain their radii. So, either from outgassing or the nebular capture of gases, some super-Earths should have started out with H_2-rich atmospheres and those with high enough gravity and low enough temperatures and/or magnetic fields should be able to retain the H_2 (e.g., Pierrehumbert & Gaidos 2011). Observational detections of H_2-rich atmospheres will ultimately be needed to confirm the scenario of thin H_2-dominated atmospheres on super-Earths.

5.3. Upper Temperatures for Life

Super-Earths with H_2-dominated atmospheres can have surface temperatures hotter than Earth due to an H_2 greenhouse effect from H_2–H_2 collision-induced opacities (Borysow 2002; Pierrehumbert & Gaidos 2011). While the hypothetical planets we have described in this paper were constructed to have 1 bar atmospheres with Earth-type surface temperatures, many H_2-dominated planet atmospheres are likely to have hotter surface temperatures than Earth, even for planets orbiting beyond 1 AU from their host stars.

An important question for understanding the potential of biosignature gases on a planet with an H_2-dominated atmospheres is therefore "how hot can a planet be and still sustain life?" On Earth, organisms that grow at 395 K are known (Lovley & Kashefi 2003; Takai et al. 2008) and have been cultured in the lab at elevated pressures equal to in situ pressures. Furthermore, proteins can function at 410–420 K (Tanaka et al. 2006; Sawano et al. 2007; Unsworth et al. 2007), motivating a consensus that life at 420 K is plausible (Deming & Baross 1993; Cowan 2004).

Life might exist at temperatures even higher than 420 K. The main argument for a maximum temperature for life involves the temperature at which the basic building blocks of life (DNA, proteins, carbohydrates, and lipids) break down. Many of the component chemicals of life, including DNA, many of the amino acids that make up proteins, and many of the key metabolites that allow lifes biochemistry to function, are rapidly chemically broken down above 470 K (e.g., Cowan 2004) The maximum temperature at which life could exist therefore may lie between 420 K and 470 K.

5.4. What Surface Pressure is too High?

Many super-Earth atmospheres will be much more massive than the 1 bar atmosphere on Earth. For temperatures suitable for the existence of liquid water (see Section 5.3), the surface pressure could be as high as 1000 bar or higher (Wagner & Pruß

2002). There are three key points to show that the high surface pressures do not destroy the biosignature gases before they can reach the high atmosphere.

"Can life generate potentially detectable biosignature gases under a massive atmosphere?" The answer is yes, provided that the surface temperature is compatible with life. Then, in principle, life can survive and generate biosignature gases. The chemistry described in this paper still holds under a massive atmosphere, because the photochemical destruction occurs above 1 mbar. Furthermore, we showed in Seager et al. (2012) that the biomass surface density estimates are unchanged under a massive atmosphere as long as the photochemical loss rate dominates. For biosignature gases whose loss is dominated by deposition at the surface (i.e., are absorbed by the surface), then the biosignature source flux and hence biomass surface density will scale linearly with the planetary atmosphere mass.

The second key question is "can the high density and pressures on the surface under a massive atmosphere generate false positives?" The answer is almost entirely no, because we have shown that it is largely the Type III biosignature gases that are viable biosignature candidates. Recall that Type III gases are those produced for reasons other than energy extraction, and not from chemicals in the environment. Therefore, they are unlikely to be the product of nonbiological chemistry, a statement that holds even under a massive atmosphere. A comment related to NH_3 potential false positive is in order. For NH_3 to be generated from N_2 and H_2 kinetically, the temperature has to be well above any temperature compatible with life for any pressure where water is liquid, extrapolating from the known fact that at 300 bar and 673 K N_2 and H_2 still need a catalyst to be converted to NH_3 and higher pressures should not change this. The false positive risk is instead in detecting NH_3 without being able to identify the surface as cold enough not to possibly generate NH_3 kinetically.

The third key question is "will the high surface pressures enable fast chemical reactions that destroy the biosignature gases generated at the surface?" The answer is no, for pressures under about 1000 bar. In principle, if the upward diffusion or convective motions bring the biosignature gas to higher altitudes faster than the gas is destroyed by kinetic reactions, the higher surface pressures will not interfere with biosignature gas accumulation in the atmosphere.

Up to 1000 bar, reaction rates extrapolated from low-pressure kinetic experiments should be valid to an order of magnitude. An additional caveat is that low-pressure gas kinetics are usually measured at high temperature and we are extrapolating to high pressure and low temperature. For example, at 1000 bar and 300 K, we estimate the half life of hydrogenation of CH_3Cl to be 6.0×10^{11} yr, the half life of DMS to be 3×10^{10} yr, and the halflife of N_2O to be 1×10^{20} yr. These numbers are based on thermochemical equilibrium of H_2 and H based on the relative Gibbs free energy of formation of atomic hydrogen and T and P (e.g., Borgnakke & Sonntag 2009). The overview is that there is very little free H at high pressures and low temperatures since, in the absence of UV, H atoms will be generated almost entirely thermochemically.

At pressures above 1000 bar, we are less confident that chemistry can be extrapolated even qualitatively from low-pressure experiments. By 1000 bar, most gases will have densities approaching those of their liquids. Increases in pressure will force molecules closer than their van der Waals radii, directly altering molecular orbitals and reaction pathways. Below ~1000 bar, we can consider molecules to be separate entities and we can still consider the molecules chemistry to be qualitatively similar to that of their dilute (ideal) gas state. Hence, order-of-magnitude extrapolations from low-pressure gas chemistry are justifiable.

5.5. Can we Identify Exoplanets with H_2-dominated Atmospheres That are Potentially Habitable?

Given the argument that life can generate biosignature gases on a planet with an H_2-rich atmosphere, but that the surface must have the right temperatures, how can we identify suitable planets for further study? The problem is that super-Earths are observed with a wide range of masses and sizes and we can anticipate that a range of atmosphere masses will also exist. A challenge is presented in observational atmosphere studies because we can only "see" to an optical depth of a few and this limiting optical depth can be reached well above any surface for a thick atmosphere. In many cases, surface conditions cannot be probed. Ideally, high-resolution spectra can be used to tell whether or not the atmosphere is thick or thin (i.e., whether or not one can observe down to the planetary surface), based on the shape of the spectral features, as described in detail in Benneke & Seager (2012, 2013).

We support the search for biosignature gases regardless of being able to classify a planet as habitable, because identifying biosignature gas molecules may be more readily attainable than high-spectral resolution characterization of a super-Earth atmospheric spectrum. That said, where possible, planetary radii can be used to discriminate planets worthy of follow up since those with small enough radii can be inferred as likely having thin atmospheres and those with radii large enough to have massive H_2 or H_2/He envelopes are unsuitable (Adams et al. 2008).

5.6. The UV Radiation of M Star

Biosignature gases can more easily accumulate in a low-UV radiation environment as compared with a high-UV radiation environment because the UV creates the destructive atmospheric species. We have shown this for H_2 atmospheres in this paper and Segura et al. (2005) have shown this for Earth-like planet atmospheres.

Whether or not truly UV-quiet M dwarfs exist and if UV activity is correlated with photometric stability is unclear. Recently, France et al. (2013) observed a small sample of six planet-hosting M dwarf stars with *HST* observations at far-UV and near-UV wavelengths and found none to be UV quiet. Other studies with much larger numbers of M dwarf stars are ongoing, including some with UV emission from the *Galaxy Evolution Explorer* (A. West, 2013, private communication). A general understanding is that magnetic activity, as traced by Hα in M dwarfs, decreases with age but that M dwarfs appear to have finite activity lifetimes such that the early-type M dwarfs (M0–M3) spin down quickly with an activity lifetime of about 1–2 Gyr whereas later type M dwarf stars (M5–M7) continue to spin rapidly for billions of years (West et al. 2006, 2008).

For the time being, UV (that is, the relevant FUV and EUV) radiation emitted by the stars of interest is not usually measured or theoretically known and so we have worked with three different UV radiation environments (Figure 1).

A relevant point for quiet M stars with extremely low-UV radiation (if they exist) is that false positives for biosignature gases destroyed by photolysis may also more easily accumulate. This is relevant for NH_3, for which the lifetime in our fiducial H_2 planet atmosphere for a planet orbiting a quiet M star is

about 1.4 Gyr, according to our photochemistry models. This means that the false positive risk that comes from primordial NH_3 would be high.[9] Related issues with other gases that are primarily destroyed by photolysis (and not destroyed by reactions with H and O) should be investigated.

5.7. Detection Prospects

Is there any hope that the next space telescope, *JWST* could be the first to provide evidence of biosignature gases? Yes, if–and only if–every single factor is in our favor.

First, we need to discover a pool of transiting planets orbiting nearby (i.e., bright) M dwarf stars. Second, the planet atmosphere should preferably have an atmosphere rich in molecular hydrogen to increase the planetary atmosphere scale height. Third, the M dwarf star needs to be a UV-quiet M dwarf star with little EUV radiation. Fourth, the planet must have life that produces biosignature gases that are spectroscopically active.

Several biosignature gases, if they exist, are detectable with tens of hours of *JWST* time, based on our detection metric. Although our detection metric assumes that photon noise is the limiting factor, many more detailed simulations of *JWST* detectability show that spectral features of a similar magnitude are detectable (e.g., Deming et al. 2009).

For detecting molecules using transmission spectroscopy, the background exoplanet atmosphere dominated by H_2 or CO_2 has little effect on the detectability of the biosignature gases of interest that we studied. This is because the transmission observations are better performed in the near-IR than in the mid-IR because of a higher stellar photon flux at near-IR wavelengths and the contamination effects of either the dominant CO_2 absorption or collision-induced H_2–H_2 absorption are minimal in the near-IR. As long as all of the biosignature gases of interest have features in the near-IR (see Figure 7 for the spectral features), these gases may be detected for atmospheres with any level of CO_2. The key issue here, instead of spectral contamination, is the mean molecular mass. The depth of the transmission spectral feature is one order of magnitude larger for H_2-dominated atmospheres compared with CO_2-dominated atmospheres (see the scale height in Equation (1)).

For detecting molecules via thermal emission with future direct imaging techniques, one may expect the CO_2 or H_2–H_2 contamination to be important because the thermal emission of a planet peaks in the mid-IR where CO_2 and H_2–H_2 contamination is most substantial. For individual gases, however, there are often multiple absorption bands to mitigate this issue. Similarly, a variety of wavelength ranges are usually available to choose from for the other biosignature gases of interest studied in this paper (as shown in Figures 4–7).

At this point, we conclude by emphasizing a related point that the plausibility of a specific biosignature gas depends on the planet surface gravity, atmospheric pressure, and other characteristics, because such characteristics affect which atmospheric wavelength "windows" are most favorable. Individual planets and their atmospheres should be considered on a case-by-case basis.

6. SUMMARY AND CONCLUSION

We have provided a "proof of concept" that biosignature gases can accumulate in exoplanets with thin H_2-dominated atmospheres. We used a model atmosphere including a detailed photochemistry code and also employed a biomass model estimate to assess plausibility of individual biosignature gases. We considered a fiducial super-Earth of $10\,M_\oplus$ and $1.75\,R_\oplus$ with a 1 bar atmosphere predominantly composed of 90% H_2 and 10% N_2 by volume and semi-major axes compatible with habitable surface temperatures. Although deviations from our fiducial model will yield different spectral features, atmospheric concentrations, etc., the main findings summarized here will still hold.

Our major finding is that for H_2-rich atmospheres, low-UV radiation environments are more favorable for biosignature gas accumulation than high-UV radiation environments. Specifically, H is the dominant reactive species generated by photochemistry in an H_2-rich atmosphere. In atmospheres with high levels of CO_2, atomic O will be the dominant destructive species for some molecules. The low-UV environments of UV-quiet M stars are favorable for the accumulation of biosignature gases in an H_2-dominated atmosphere. The high-UV environment of Sun-like and active M dwarf stars largely prevents biosignature gas accumulation due to rapid photochemical destruction via H (or sometimes O), where its concentration is controlled by UV photolysis. High-UV radiation is also unfavorable for the accumulation of biosignature gases in oxidized atmospheres (Segura et al. 2005), although, in contrast, OH is the main reactive species in oxidized atmospheres.

We investigated the plausibility of a number of biosignature gases, including H_2, CH_4, H_2S, DMS, NH_3, N_2O, NO, CH_3Cl, and HCl. While not exhaustive, we came up with some plausible biosignature gases and others that are unsuitable as biosignature gases, as follows.

Our list of plausible biosignature gases is dominated by Type III biosignature gases in low-UV environments. These include CH_3Cl, DMS, and N_2O. Type III gases are gases produced for specialized functions and therefore could well include small molecules as yet unknown. We therefore support the idea of searching for high concentrations of gases that do not belong in chemical equilibrium.

We also presented a new biosignature gas candidate, NH_3, the only one we found to be a reasonable Type I biosignature gas candidate, and one unique to a hydrogen-rich environment. Type I gases are gases produced as by-products from energy extraction from the environment.

Our list of unlikely biosignature gases is dominated by Type I biosignature gases, as any biosignature gases produced from energy extraction (such as CH_4 or H_2S and numerous others) will be either be produced by geochemical or photochemical processes or likely rapidly destroyed by hydrogenation in a hydrogen-dominated environment.

We have not identified any unique biosignature gas produced by any type of photosynthesis in a thin H_2-rich atmosphere comparable with O_2 in oxidized atmospheres. In an H_2-dominated environment, the most likely photosynthetic by-product is molecular hydrogen, already prevalent in the H_2-dominated atmosphere, or non-volatile mineral products. This is in contrast with the O_2 produced by photosynthesis in oxidized environments that is quite robust to most false positive scenarios. (We call biosignature gases from biomass building Type II.)

Bioindicators would be helpful, but are not easily or uniquely detectable. The examples we gave were the hydrogen halides.

Overall, the promise of biosignature gases in H_2 atmospheres is real. We have aimed to provide a conceptual and quantitative

[9] NH_3 requires on average two photons for destruction, hence its UV lifetime is particularly sensitive to UV levels.

framework to show that there are at least some viable biosignature gases that could be produced either by life's capture of environmental chemical energy or are in a category of gases produced by terrestrial life. We intend for the results here to fuel the motivation for discovery of habitable Earths and super-Earths orbiting M dwarf stars and their atmospheric follow up with *JWST*.

We thank Jean-Michel Desert and Kartik Sheth for motivating questions. We thank the Foundational Questions Institute (FQXI) for funding the seeds of this work many years ago.

REFERENCES

Adams, E. R., Seager, S., & Elkins-Tanton, L. 2008, ApJ, 673, 1160
Allard, F., Hauschildt, P. H., Alexander, D. R., & Starrfield, S. 1997, ARA&A, 35, 137
Amend, J. P., & Shock, E. L. 2001, FEMS Microbiol. Rev., 25, 175
Bains, W., & Seager, S. 2012, AsBio, 12, 271
Banks, P. M., & Kockarts, G. 1973, Aeronomy (New York: Academic)
Benneke, B., & Seager, S. 2012, ApJ, 753, 100
Benneke, B., & Seager, S. 2013, ApJ, in press (arXiv:1306.6325)
Borgnakke, C., & Sonntag, R. E. 2009, Fundamentals of Thermodynamics (New Jersey: Wiley)
Borysow, A. 2002, A&A, 390, 779
Cowan, D. A. 2004, Trends Microbiol., 12, 58
Deming, D., Seager, S., Winn, J., et al. 2009, PASP, 121, 952
Deming, D., Wilkins, A., McCullough, P., et al. 2013, ApJ, 774, 95
Deming, J. W., & Baross, J. A. 1993, GeCoA, 57, 3219
Des Marais, D. J., Harwit, M. O., Jucks, K. W., et al. 2002, AsBio, 2, 153
Domagal-Goldman, S. D., Meadows, V. S., Claire, M. W., & Kasting, J. F. 2011, AsBio, 11, 419
Elkins-Tanton, L. T., & Seager, S. 2008, ApJ, 685, 1237
France, K., Froning, C. S., Linsky, J. L., et al. 2013, ApJ, 763, 149
Friend, A. D., Geider, R. J., Behrenfeld, M. J., & Still, C. J. 2009, in Photosynthesis in Silico: Understanding Complexity from Molecules to Ecosystem., ed. A. Laisk, L. Nedbal, & B. V. Govindjee (Dordrecht, The Netherlands: Springer), 465
Gardner, J. P., Mather, J. C., Clampin, M., et al. 2006, SSRv, 123, 485
Glindemann, D., Edwards, M., Liu, J. A., & Kuschk, P. 2005, Ecol. Eng., 24, 457
Hitchcock, D. R., & Lovelock, J. E. 1967, Icar, 7, 149
Hu, R. 2013, PhD thesis, MIT
Hu, R., Seager, S., & Bains, W. 2012, ApJ, 761, 166
Hu, R., Seager, S., & Bains, W. 2013, ApJ, 769, 6
Kaltenegger, L., & Traub, W. A. 2009, ApJ, 698, 519
Lammer, H., Güdel, M., Kulikov, Y., et al. 2012, EP&S, 64, 179
Lawson, P. R., Lay, O. P., Martin, S. R., et al. 2008, Proc. SPIE, 7013, 70132N
Lederberg, J. 1965, Natur, 207, 9
Lovelock, J. E. 1965, Natur, 207, 568
Lovley, D. R., & Kashefi, K. 2003, Sci, 301, 934
Madhusudhan, N., & Seager, S. 2009, ApJ, 707, 24
Mentall, J. E., & Gentieu, E. P. 1970, JChPh, 52, 5641
Miller-Ricci, E., Seager, S., & Sasselov, D. 2009, ApJ, 690, 1056
Nishibayashi, Y., Iwai, S., & Hidai, M. 1998, Sci, 279, 540
Pierrehumbert, R., & Gaidos, E. 2011, ApJL, 734, L13
Pilcher, C. B. 2003, AsBio, 3, 471
Prinn, R. G., & Olaguer, E. P. 1981, JGR, 86, 9895
Roels, J., & Verstraete, W. 2001, Bioresour. Technol., 79, 243
Rothman, L. S., Gordon, I. E., Barbe, A., et al. 2009, JQSRT, 110, 533
Sander, S. P., Friedl, R. R., Abbatt, J. P. D., et al. 2011, Chemical Kinetics and Photochemical Data for Use in Atmospheric Studies, Evaluation Number 17 (JPL Publication 10-6; Pasadena, CA: JPL)
Sawano, M., Yamamoto, H., Ogasahara, K., et al. 2007, Biochemistry, 47, 721
Schaefer, L., & Fegley, B. 2010, Icar, 208, 438
Schrock, R. R. 2011, NatCh, 3, 95
Seager, S. 2010, Exoplanet Atmospheres: Physical Processes (Princeton, NJ: Princeton Univ. Press)
Seager, S. 2013, Sci, 340, 577
Seager, S., Bains, W., & Hu, R. 2013, ApJ, 775, 104
Seager, S., Kuchner, M., Hier-Majumder, C. A., & Militzer, B. 2007, ApJ, 669, 1279
Seager, S., & Sasselov, D. D. 2000, ApJ, 537, 916
Seager, S., Schrenk, M., & Bains, W. 2012, AsBio, 12, 61
Seager, S., Whitney, B. A., & Sasselov, D. D. 2000, ApJ, 540, 504
Segura, A., Kasting, J. F., Meadows, V., et al. 2005, AsBio, 5, 706
Seinfeld, J. H., & Pandis, S. N. 2000, Atmospheric Chemistry and Physics: From Air Pollution to Climate Change (Hoboken, NJ: Wiley)
Shin, K., Kumar, R., Udachin, K. A., Alavi, S., & Ripmeester, J. A. 2012, PNAS, 109, 14785
Solomon, S., Qin, D., Manning, M., et al. 2007, Contribution of Working Group I to the Fourth Assessment Report of the Intergovernmental Panel on Climate Change (Cambridge: Cambridge Univ. Press)
Takai, K., Nakamura, K., Toki, T., et al. 2008, PNAS, 105, 10949
Tanaka, T., Sawano, M., Ogasahara, K., et al. 2006, FEBS Lett., 580, 4224
Tijhuis, L., van Loosdrecht, M. C. M., & Heijnen, J. J. 1993, Biotechnol. Bioeng., 42, 509
Unsworth, L. D., van der Oost, J., & Koutsopoulos, S. 2007, FEBS J., 274, 4044
Wagner, W., & Pruß, A. 2002, JPCRD, 31, 387
Wang, J. S., Logan, J. A., McElroy, M. B., et al. 2004, GBioC, 18, GB3011
West, A. A., Bochanski, J. J., Hawley, S. L., et al. 2006, AJ, 132, 2507
West, A. A., Hawley, S. L., Bochanski, J. J., et al. 2008, AJ, 135, 785
Yandulov, D. V., & Schrock, R. R. 2003, Sci, 301, 76